

Molecular Dynamics of the *Shewanella oneidensis* Response to Chromate Stress*[§]

Steven D. Brown^{‡§}, Melissa R. Thompson^{§¶||**}, Nathan C. VerBerkmoes[¶],
Karuna Chourey[‡], Manesh Shah^{‡‡}, Jizhong Zhou[‡], Robert L. Hettich^{¶§§},
and Dorothea K. Thompson^{‡¶|||}

Temporal genomic profiling and whole-cell proteomic analyses were performed to characterize the dynamic molecular response of the metal-reducing bacterium *Shewanella oneidensis* MR-1 to an acute chromate shock. The complex dynamics of cellular processes demand the integration of methodologies that describe biological systems at the levels of regulation, gene and protein expression, and metabolite production. Genomic microarray analysis of the transcriptome dynamics of midexponential phase cells subjected to 1 mM potassium chromate (K_2CrO_4) at exposure time intervals of 5, 30, 60, and 90 min revealed 910 genes that were differentially expressed at one or more time points. Strongly induced genes included those encoding components of a TonB1 iron transport system (*tonB1-exbB1-exbD1*), heme ATP-binding cassette transporters (*hmuTUV*), TonB-dependent receptors as well as sulfate transporters (*cysP*, *cysW-2*, and *cysA-2*), and enzymes involved in assimilative sulfur metabolism (*cysC*, *cysN*, *cysD*, *cysH*, *cysI*, and *cysJ*). Transcript levels for genes with annotated functions in DNA repair (*lexA*, *recX*, *recA*, *recN*, *dinP*, and *umuD*), cellular detoxification (*so1756*, *so3585*, and *so3586*), and two-component signal transduction systems (*so2426*) were also significantly up-regulated ($p < 0.05$) in Cr(VI)-exposed cells relative to untreated cells. By contrast, genes with functions linked to energy metabolism, particularly electron transport (e.g. *so0902-03-04*, *mtrA*, *omcA*, and *omcB*), showed dramatic temporal alterations in expression with the majority exhibiting repression. Differential proteomics based on multidimensional HPLC-MS/MS was used to complement the transcriptome data, resulting in comparable induction and repression patterns for a subset of corresponding proteins. In total, expression of 2,370 proteins were confidently verified with 624 (26%) of these annotated as hypothetical or conserved hypothetical proteins. The initial response of *S. oneidensis* to chromate shock appears to require a combination of different regulatory networks

that involve genes with annotated functions in oxidative stress protection, detoxification, protein stress protection, iron and sulfur acquisition, and SOS-controlled DNA repair mechanisms. *Molecular & Cellular Proteomics* 5: 1054–1071, 2006.

Hexavalent chromium [Cr(VI)], in the form of chromate (CrO_4^{2-}) or dichromate ($Cr_2O_7^{2-}$) species, is a serious anthropogenic pollutant found in the discharged effluents from various manufacturing and military industries (1, 2) and is one of several risk-driving contaminants found at unacceptable levels in groundwater as well as soil and sediment at the United States Department of Energy waste sites (3). The most chemically stable and common forms of chromium in the environment are the trivalent Cr(III) and hexavalent Cr(VI) species, which differ significantly in their physicochemical properties and biological responsiveness (*i.e.* toxicity). Cr(VI) is highly soluble and a toxic non-essential metal for most organisms with chronic chromate exposure leading to mutagenesis and carcinogenesis, whereas Cr(III) is sparingly soluble and relatively innocuous (4–6).

In situ microbial bioreduction of Cr(VI) to Cr(III) is of particular interest because it may serve as a potential strategy for the detoxification and immobilization of chromate compared with more cost-prohibitive physical and chemical treatment methods (7). Microorganisms exhibiting Cr(VI)-reducing activities and resistance have been detected in chromate-contaminated sites as well as natural, uncontaminated ecosystems (8–10). Previous studies have indicated that species of the γ -proteobacterial genus *Shewanella* are capable of both direct (enzymatic) dissimilatory Cr(VI) reduction (11–13) and indirect (chemical) Cr(VI) reduction driven by the reduction of Fe(III) to Fe(II) (14–16). Myers *et al.* (12) demonstrated that formate-dependent Cr(VI) reductase activity was localized to the cytoplasmic membrane of anaerobically grown *Shewanella oneidensis* MR-1 (previously named *Shewanella putrefaciens* MR-1). Similarly chromate reductase activity was shown to be preferentially associated with the membrane fraction of *Enterobacter cloacae* cells (17), whereas soluble Cr(VI)-reducing enzymes have been purified to varying degrees from *Pseudomonas putida* MK1 (18), *P. putida* PRS2000 (19), and *Pseudomonas ambigua* G-1 (20). Reductases with other primary cellular functions have been shown

From the [‡]Environmental Sciences Division, [¶]Chemical Sciences Division, and ^{‡‡}Life Sciences Division, Oak Ridge National Laboratory, Oak Ridge, Tennessee 37831, ^{||}Graduate School of Genome Science and Technology, University of Tennessee-Oak Ridge National Laboratory, Tennessee 37830, and ^{¶¶}Department of Biological Sciences, Purdue University, West Lafayette, Indiana 47907

Received, December 5, 2005, and in revised form, February 27, 2006

Published, MCP Papers in Press, March 8, 2006, DOI 10.1074/mcp.M500394-MCP200

to be efficient in chromate reduction (21), suggesting that a variety of enzymes may participate in the transfer of electrons to Cr(VI). Studies investigating the effect of nitrite on hexavalent chromium reduction indicated that *S. oneidensis* MR-1 might possess multiple nonspecific Cr(VI) reduction mechanisms, as well as metal resistance mechanisms, that are dependent on physiological growth conditions (13).

Oxidatively induced DNA damage is considered to be the basis of chromate genotoxicity (22–24) with active transport of chromate across biological membranes being mediated by the sulfate transport system in prokaryotic and eukaryotic cells (7, 25, 26). The chromate resistance mechanisms displayed by microorganisms are diverse and include biosorption, diminished intracellular accumulation through either direct obstruction of the ion uptake system or active chromate efflux, precipitation, and reduction of Cr(VI) to less toxic Cr(III) (for a review, see Ref. 7). Plasmid-determined resistance to chromate has been shown to occur in bacteria, including species of the genera *Pseudomonas* (27–29) and *Alcaligenes* (25). A hydrophobic protein, designated ChrA, was found to be responsible for the plasmid-specified resistance phenotype in these organisms (30, 31) and appears to function as a secondary transport system for the extrusion of chromate ions (32). Although Cr(VI) reduction and toxicity resistance mechanisms are considered to be unlinked cellular processes, the biotransformation of Cr(VI) to Cr(III) likely contributes to the detoxification of chromate (33, 34).

The goal of the study described here was to obtain global insight into temporal alterations in mRNA expression and protein synthesis that occur in response to toxic acute levels of chromate and thus to gain an understanding of the potential molecular mechanisms enabling Cr(VI) detoxification under aerobic respiratory conditions. For the most part, the observed alterations in the protein patterns reflected the changes identified at the transcriptomic level. In addition, differential proteomics revealed post-transcriptional levels of regulation that cannot be captured by microarray analysis. The combined transcriptome and proteome analyses suggested a close relationship between chromate stress and cellular iron requirement (or limitation) as indicated by the dramatic induction of genes involved in iron sequestration and uptake. Sulfate transport and assimilatory pathways for cysteine production, DNA damage repair systems, and oxidative stress protection were also major features of the initial response of *S. oneidensis* MR-1 to acute Cr(VI) exposure. The present study identified a number of genes and their encoded products that have been shown previously to be important for the oxidative stress response of MR-1 (35) and other bacteria. Moreover a number of other genes/proteins not described previously were implicated in the cellular detoxification of chromate. This study represents an essential first step toward a global molecular characterization of the cellular response to acute chromate exposure in a metal-reducing bacterium and provides information necessary

for future examination of metal stress-linked gene regulatory networks.

EXPERIMENTAL PROCEDURES

Bacterial Strains, Culture Conditions, and Assays—*S. oneidensis* strain MR-1 (36) was used for both transcriptomic and proteomic analyses and was propagated in Luria-Bertani (LB)¹ medium (pH 7.2) at 30 °C under aerobic conditions. A Bioscreen C microbiological culture system (Growth Curves USA, Piscataway, NJ) was used to monitor the growth of MR-1 in response to different concentrations of K₂CrO₄ over 48 h. Chromate reduction was measured using the 1,5-diphenylcarbazide method essentially as described previously (18).

RNA Isolation and Preparation of Fluorescein-labeled cDNA—For the time series microarray experiment, a 1:1000 dilution of a fresh overnight culture (16 h) of *S. oneidensis* MR-1 was used to inoculate prewarmed LB medium in six 250-ml sidearm Pyrex flasks. Batch cultures were grown to midexponential phase (A_{600} , 0.5) followed by the addition of prewarmed 2 M K₂CrO₄ to a final concentration of 1 mM for three of the six cultures. The remaining three cultures served as the reference (control) samples and were grown in parallel with the treated cells. For microarray hybridization, the control and treated cells were harvested in parallel for total cellular RNA extraction at 5, 30, 60, and 90 min post-K₂CrO₄ addition. RNA isolation, fluorescent labeling reactions, probe purification, and microarray hybridization were performed as described previously (37).

Microarray Hybridization, Scanning, Image Quantification, and Data Analysis—*S. oneidensis* MR-1 microarray construction, hybridization, scanning, image quantification, and data analyses were performed as described previously (38, 39). Briefly temporal gene expression analysis was performed using six microarrays for each time point (three biological replicates × two dye reversal reactions) with each slide containing two spots representing each gene at different array locations for a total of 12 signal intensity measurements per gene per time point. The two separately labeled cDNA pools (*i.e.* the K₂CrO₄-treated and the corresponding control time point) to be compared were mixed together in a hybridization solution containing 50% (v/v) formamide. Microarray hybridization signals were quantified using ImageGene Version 5.5 (Biodiscovery, Inc., Los Angeles, CA) followed by data transformation and normalization using GeneSite Light (Biodiscovery, Inc.). ArrayStat™ (Imaging Research, Inc., Ontario, Canada) was used to determine the common error of these values, remove outliers, and determine statistical significance via a z test for two independent conditions and the false discovery rate method (nominal α , $p < 0.05$). Genes exhibiting significant changes in expression at a degree of 2-fold or greater (40) were further analyzed using the program Hierarchical Clustering Explorer Version 3.0 (www.cs.umd.edu/hcil/multi-cluster/).

Real Time Quantitative RT (QRT)-PCR Analysis—Microarray data were validated using real time QRT-PCR as described previously (39) except that iQ SYBR Green Supermix (Bio-Rad) was used according to the manufacturer's instructions instead of SYBR Green I. Six genes representing the range of induced to unchanged gene expression values based on microarray hybridization were analyzed for the four time points of Cr(VI) exposure using real time QRT-PCR. The following genes were selected for comparative QRT-PCR analysis, and primer pairs (given in parentheses) were designed using the program Primer3 (www-genome.wi.mit.edu/cgi-bin/primer/primer3_www.cgi): *tonB2* (5'-CAAAGGGTCTGACCTCAACC, 3'-GAACGACATTGCCGTATC-

¹ The abbreviations used are: LB, Luria-Bertani; QRT, quantitative RT; ROS, reactive oxygen species; 2-D, two-dimensional; LTQ, linear trapping quadrupole; ABC, ATP-binding cassette.

AA, so2426 (5'-GCAGAAGGATTTAGGTCGAT, 3'-CGGTGTTGATTAAGTACGC), so3032 (5'-GATTCTATCCGAGTACCAG, 3'-CAAGAGGGTTTCACTTATGC), so3585 (5'-CGAGGCTATCCATCACTTAG, 3'-ACCTTTTGTGCTATTCTGG), tonB1 (5'-CAGGGTGAATCACATCAACG, 3'-TAACAGCGTTACGAGCAGCA), and *exbB1* (5'-CATTCTCGCCTTGATGATT, 3'-GGCGTAGCTCTTTAACCCAAG).

Preparation of Proteomes for HPLC-MS/MS Analysis—All chemical reagents were obtained from Sigma unless stated otherwise. Modified sequencing grade trypsin (Promega, Madison, WI) was used in all digestions. HPLC grade water and acetonitrile were acquired from Burdick & Jackson (Muskegon, MI), and 99% formic acid was purchased from EM Science (Darmstadt, Germany).

For large scale proteomic characterization, 500-ml cultures of *S. oneidensis* MR-1 in 4-liter flasks (a total of 1 liter of culture for treatment and control) were grown to midexponential phase (A_{600} , 0.5) under the same conditions as described above for the microarray studies and then either exposed to a final K_2CrO_4 concentration of 1 mM or allowed to continue growing in the absence of added chromate. At time points of 45 and 90 min after treatment with K_2CrO_4 , cells were harvested from each of the following conditions for HPLC-MS/MS analysis: 1) Control 1 (untreated midlog phase cells after 45 min of further growth), 2) Treatment 1 (45 min post-Cr addition), 3) Control 2 (untreated midlog phase cells after 90 min of further growth), and 4) Treatment 2 (90 min post-Cr addition). For this, cells were pelleted by centrifugation ($5,000 \times g$ for 5 min), resuspended in ice-cold LB medium, washed two times in 50 mM Tris, 10 mM EDTA (pH 7.6), and centrifuged at $5,000 \times g$ for 10 min. The *S. oneidensis* cells were then placed on ice and lysed by sonication using a microprobe at high power with 30-s pulses for five times with a 30-s cooling period between each sonication. Cellular debris were removed by centrifugation at $5,000 \times g$ for 10 min. The supernatant was centrifuged at $100,000 \times g$ for 60 min in an ultracentrifuge to separate a soluble fraction from a pellet. The pellet (membrane fraction) was washed with 50 mM Tris, 10 mM EDTA (pH 7.6) and centrifuged at $100,000 \times g$ for 60 min; this fraction was then resuspended in 50 mM Tris, 10 mM EDTA (pH 7.6) by brief sonication. Both proteome fractions were quantified using bicinchoninic acid (BCA) analysis, aliquoted, and stored at $-80^\circ C$ until ready for digestion. Approximately 2 mg of each proteome fraction (soluble and membrane) prepared for the two growth conditions was denatured and reduced in 6 M guanidine and 10 mM DTT ($60^\circ C$ for 1 h). The denatured/reduced proteome mixture was diluted 6-fold with 50 mM Tris, 10 mM $CaCl_2$ (pH 7.8), and sequencing grade trypsin was added at 1:100 (protease/protein (w/w)). The digestions were run with gentle shaking at $37^\circ C$ for 18 h followed by a second addition of trypsin at 1:100 and an additional 5 h incubation. The samples were treated with 20 mM DTT for 1 h at $37^\circ C$ as a final reduction step to remove remaining disulfide bonds and then immediately desalted using Sep-Pak Plus C_{18} solid phase extraction (Waters, Milford, MA). All samples were concentrated and solvent-exchanged into 0.1% formic acid in water by centrifugal evaporation to $\sim 10 \mu g/\mu l$ starting material, filtered, aliquoted, and stored at $-80^\circ C$ until ready for LC-MS/MS analysis.

LC/LC-MS/MS Analysis—The proteome fractions (soluble and membrane) prepared from control and chromate-treated samples were analyzed in duplicate via two-dimensional (2-D) LC-MS/MS experiments using an Ultimate HPLC system (LC Packings, a division of Dionex, San Francisco, CA) coupled to a linear trapping quadrupole (LTQ) mass spectrometer (ThermoFinnigan, San Jose, CA). The HPLC pump provided a flow rate of $\sim 100 \mu l/min$ that was split precolumn to achieve a final flow rate of $\sim 200 nl/min$ at the nanospray tip. A split phase column (150- μm inner diameter fused silica) was packed via a pressure cell as follows: ~ 3.5 cm of strong cation exchange (Luna SCX, 5 μm , 100 \AA ; Phenomenex, Torrance, CA) followed by ~ 3.5 cm of C_{18} reverse phase (Aqua C_{18} , 5 μm , 200 \AA ; Phenomenex). Subse-

quently $\sim 500 \mu g$ of sample was loaded onto the split phase column via a pressure cell. The loaded split phase column was then inserted behind a PicoFrit tip (100- μm inner diameter, 15- μm inner diameter at the tip; New Objective, Woburn, MA) packed via a pressure cell with ~ 15 cm of C_{18} reverse phase (Jupiter C_{18} , 5 μm , 300 \AA ; Phenomenex). This entire column system was positioned in front of the LTQ on a nanospray source (ThermoFinnigan).

All samples were analyzed via a 24-h 12-step 2-D analysis consisting of increasing concentration (0–500 mM) salt pulses of ammonium acetate followed by 2-h reverse phase gradients from 100% aqueous solvent (95% H_2O , 5% ACN, 0.1% formic acid) to 50% organic solvent (30% H_2O , 70% ACN, 0.1% formic acid). During the entire chromatographic process, the LTQ was operated in a data-dependent MS/MS mode detailed below. The chromatographic methods and HPLC columns were identical for all analyses. The LC-MS/MS system was fully automated and under direct control of the Xcalibur software system (ThermoFinnigan). The LTQ was operated with a nanospray voltage of 2.6 kV, heated capillary temperature of $200^\circ C$, and a full scan m/z range of 400–1700. Data-dependent MS/MS mode was operated as follows. Five MS/MS spectra were acquired following every full scan, two microscans were averaged for every full MS and MS/MS spectra, a 3 m/z isolation width was used, and 35% collision energy was used for fragmentation. The dynamic exclusion was set to 1 with an exclusion duration of 3 min.

Proteome Bioinformatics—A protein database was created by combining the most recent version of the *S. oneidensis* MR-1 database (Version 8; www.tigr.org/) containing a total of 4,798 predicted proteins with 36 common contaminants (trypsin, keratin, etc.). The database can be downloaded from the website compbio.ornl.gov/shewanella_chromium_stress/databases/. For all database searches, the MS/MS spectra were searched using SEQUEST (Ref. 41; ThermoFinnigan) with the following parameters: enzyme type, trypsin; parent mass tolerance, 3.0; fragment ion tolerance, 0.5; up to four missed cleavages allowed; fully tryptic peptides only. The MS/MS spectra from individual RAW files were first converted to mzXML format by using ReAdW software written at the Institute for Systems Biology in Seattle, WA (www.systemsbio.org) and can be downloaded from the SourceForge repository (sashimi.sourceforge.net). Individual spectra were then converted to DTA files by mzXML2Other, also from the Institute for Systems Biology. DTA files are the required format for input into SEQUEST (see Ref. 52). The output data files were then filtered and sorted with the DTASelect algorithm (42) using the following parameters: fully tryptic peptides only with ΔCN of at least 0.08 and cross-correlation scores (Xcorr) of at least 1.8 (+1), 2.5 (+2), and 3.5 (+3). These threshold scores have been tested rigorously in our laboratory and provide a high confidence of identification (see Refs. 43 and 52 for more discussion) with a maximum false-positive rate of 1–2%. Post-translational modifications and other fixed modifications (i.e. due to addition of iodoacetamide) were not included in the search parameters. DTASelect files are available on the analysis page (compbio.ornl.gov/shewanella_chromium_stress/ms_analysis) under the corresponding dataset and are filtered at one peptide and two peptides per protein. The files are presented in a text format or a viewable html version where every identified spectrum can be viewed by clicking on the spectral number (first column, labeled by filename). The DTASelect results from all control and chromate-treated samples were then compared with the Contrast program (42) for each time point. These results are located under the global contrast heading on the analysis page. A list was made of all proteins showing a reproducible significant change of at least 40% sequence coverage, five or more unique peptides, and/or a reproducible spectral count difference of $2 \times$ between the control and chromate-treated samples at each time point (adapted from Refs. 39 and 43). The analysis page also contains inter-run contrast files

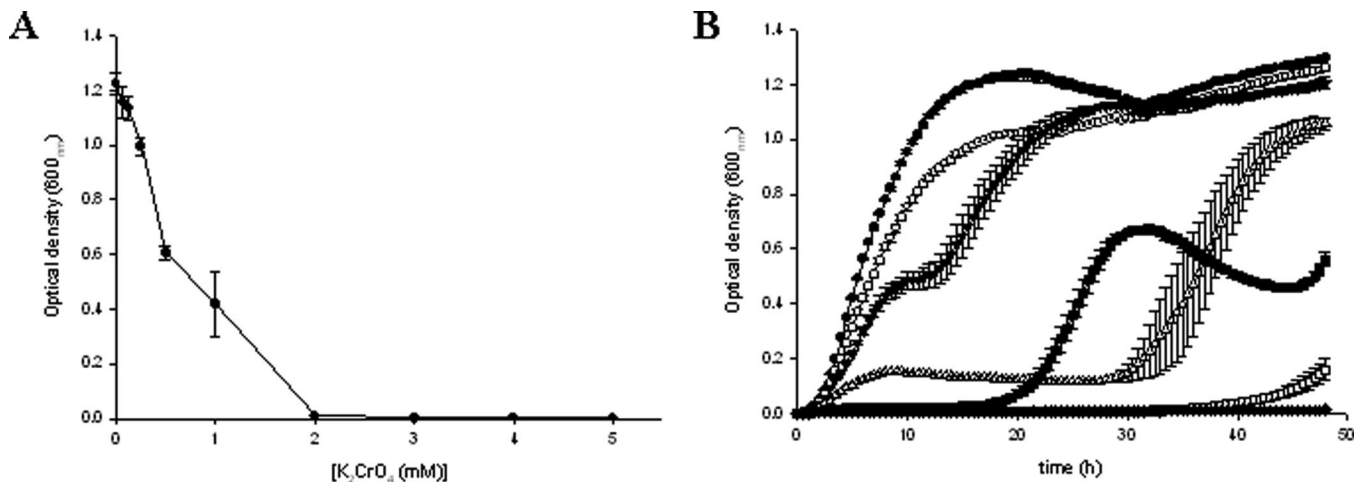


FIG. 1. Dose-response growth curves describing the toxicity of potassium chromate (K_2CrO_4) for *S. oneidensis* strain MR-1. A, the minimal inhibitory concentration of K_2CrO_4 for MR-1 determined in LB broth under aerobic growth conditions at 30 °C after 48 h. B, growth curves of MR-1 over 48 h in LB medium containing the following final concentrations of K_2CrO_4 were measured using a Bioscreen C apparatus: 0 mM (●), 0.0625 mM (○), 0.125 mM (▼), 0.25 mM (△), 0.5 mM (■), 1 mM (□), and 2 mM (◆). The mean $A_{600} \pm$ S.E. (bars) for three replicate growth point measurements is shown, and three independent experiments were conducted.

(compares duplicate runs on same sample) as well as fractionation comparisons (compares replicate runs of the same proteome broken down by fraction).

RESULTS

Physiological Effect of Chromate during Aerobic Growth of *S. oneidensis*—Initially we investigated the effects of chromate-induced stress on the growth of aerobically growing cultures of *S. oneidensis* MR-1 to identify adequate concentrations for transcriptome and proteome analyses. Three independent experiments based on end point culture turbidity determinations indicated that MR-1 responded to K_2CrO_4 in a dose-dependent manner. MR-1 cells that were grown in the presence of 0.06 and 0.125 mM Cr(VI) attained A_{600} values similar to those attained for cells grown in the absence of heavy metal in the medium after 48 h (Fig. 1A). MR-1 cultured with 0.25, 0.5, and 1 mM K_2CrO_4 showed ~17, 50, and 66% reductions in growth, respectively. Culture turbidity did not increase for inocula in medium containing 2 mM K_2CrO_4 after 48 h.

To provide a complete description of the growth behavior exhibited by MR-1 in response to different amounts of Cr(VI), culture turbidity was measured at 30-min intervals under aerobic conditions over the course of 48 h using a Bioscreen C reader. As shown in Fig. 1B, growth rates of MR-1 in the presence of 0.06 and 0.125 mM K_2CrO_4 were decreased slightly relative to growth in the absence of added K_2CrO_4 , but similar maximal turbidity measurements were obtained after 48 h. Extended lag periods, ranging from 20–40 h, followed by biphasic growth with a period of growth arrest and then by complete or partial recovery were observed for MR-1 grown in LB medium containing higher Cr(VI) concentrations (*i.e.* 0.25, 0.5, and 1 mM; Fig. 1B). However, MR-1 was unable to grow after 48 h in 2 mM K_2CrO_4 under the conditions tested in the present study (Fig. 1B).

Chromate Reduction—A chromate concentration of 1 mM was selected for global gene and protein expression profiling. To determine whether chromate reduction occurs in the presence of exponentially growing *S. oneidensis* cells upon addition of 1 mM K_2CrO_4 , a spectrophotometric method using 1,5-diphenylcarbazide (18) was used to monitor chromate conversion over the entire time course of the transcriptome and proteome analyses. No chromate disappearance was observed for Cr(VI)-shocked midlog phase cells over a 150-min period (see Supplemental Fig. S1). Similarly no abiotic conversion of chromate was detected in the LB broth-only control (Supplemental Fig. S1), thus eliminating the possible contribution of Fe^{3+} in the chemical reduction of chromate. After 24 h of incubation in LB medium containing 1 mM K_2CrO_4 , wild-type MR-1 cells transformed ~42% of Cr(VI) (results not shown).

General Transcriptome Dynamic Patterns in Response to Chromate Shock and Array Data Validation—To define the repertoire and temporal expression patterns of MR-1 genes responding to acute Cr(VI) exposure (1 mM K_2CrO_4), transcriptome dynamics were examined based on time series DNA microarray experiments at 5, 30, 60, and 90 min postshock using whole-genome microarrays. Temporal gene expression profiles of cells exposed to Cr(VI) were compared with those of the untreated control cells grown in parallel. Approximately 20% ($n = 910$) of the total predicted *S. oneidensis* genes ($n = 4,648$) represented on the microarray showed at least a 2-fold statistically significant ($p < 0.05$) change in expression for at least one of the time points during acute Cr(VI) stress exposure. Generally the number of up- and down-regulated genes increased with time of exposure to chromate. At all four time points, as many as 54 genes were induced more than 2-fold, whereas only 12 genes were repressed at all time points

S. oneidensis Chromate Stress Response

(Table I). Pairwise complete linkage clustering analysis of expression profile patterns for this subset of ORFs revealed three major clusters of genes exhibiting similar or potentially co-regulated expression patterns (see Supplemental Fig. S2 and Table S1).

Chromate-responsive genes displayed a wide distribution

TABLE I
Number of genes induced and repressed at least 2-fold in transcriptome profiling experiments at different time intervals following the addition of 1 mM potassium chromate

Time (min) after addition of 1 mM K ₂ CrO ₄	Number of genes	
	Induced	Repressed
5	147	36
30	186	164
60	202	244
90	342	293
At least one time point	483	444
All time points	54	12

among functional classes based on The Institute for Genomic Research annotations (Ref. 44; www.tigr.org, Comprehensive Microbial Resource) across the entire course of exposure (Fig. 2). The early response (5 min) was characterized predominantly by up-regulation of genes whose products mostly belonged to the functional categories of energy metabolism, hypothetical proteins, and transport/binding proteins (Fig. 2A). General expression patterns during the middle time intervals (30 and 60 min) of K₂CrO₄ exposure were characterized by a marked increase in the number of down-regulated genes in the following functional categories: biosynthesis of cofactors, prosthetic groups, and carriers; cellular processes; energy metabolism; hypothetical proteins; protein fate; purines, pyrimidines, nucleosides, and nucleotides; regulatory functions; transport and binding proteins; and proteins of unknown function (Fig. 2, B and C). For most functional groups, the maximal transcriptional response in terms of numbers of differentially expressed ORFs occurred at the 90-min (late phase) post-Cr(VI) shock time point (Fig. 2D). At this time

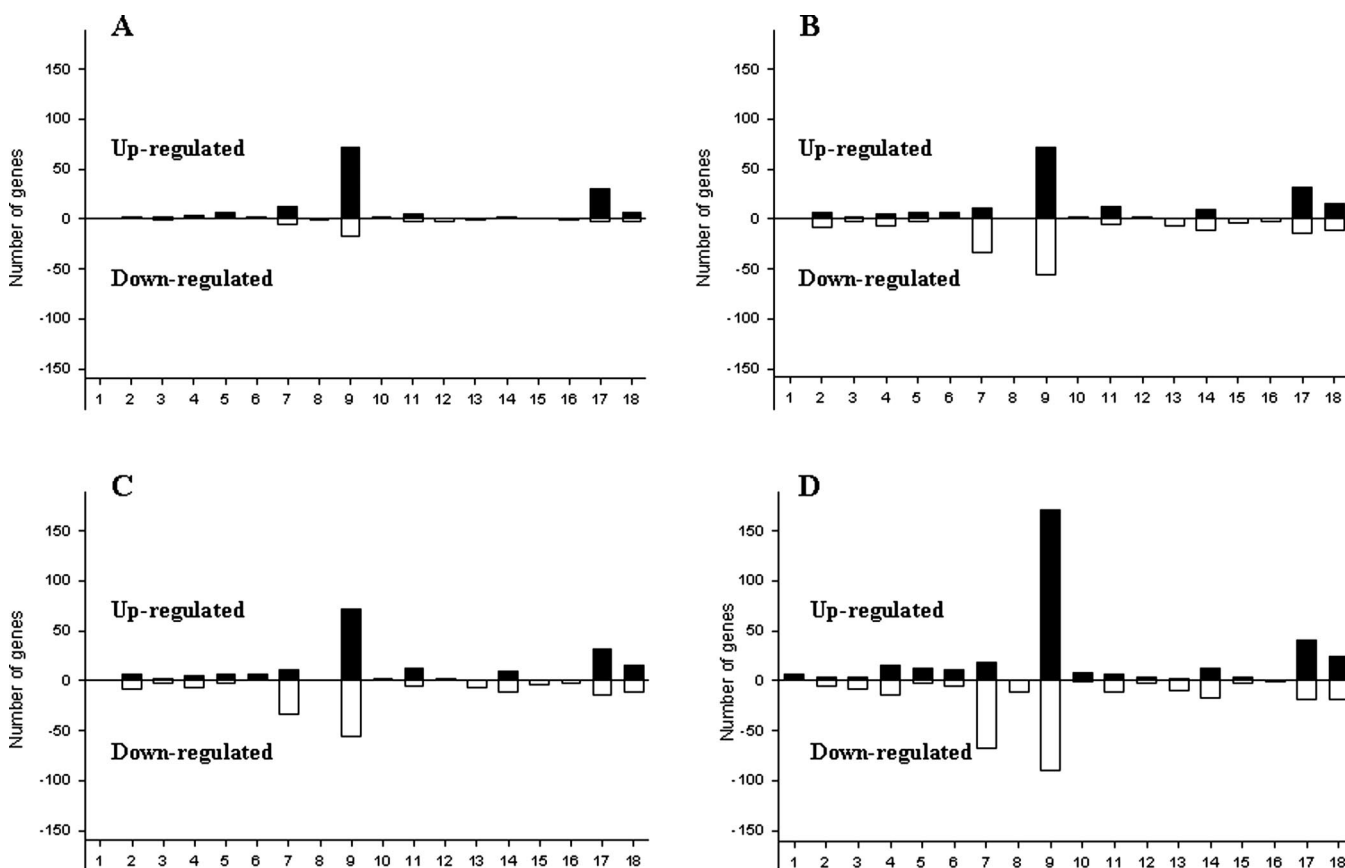


FIG. 2. Differentially expressed genes grouped by functional classification according to The Institute for Genomic Research *S. oneidensis* genome database and shown for the post-treatment time intervals of 5 (A), 30 (B), 60 (C), and 90 (D) min. Column 1, amino acid biosynthesis; column 2, biosynthesis of cofactors, prosthetic groups, and carriers; column 3, cell envelope; column 4, cellular processes; column 5, central intermediary metabolism; column 6, DNA metabolism; column 7, energy metabolism; column 8, fatty acid and phospholipid metabolism; column 9, hypothetical proteins; column 10, mobile and extrachromosomal element functions; column 11, protein fate; column 12, protein synthesis; column 13, purines, pyrimidines, nucleosides, and nucleotides; column 14, regulatory functions; column 15, signal transduction; column 16, transcription; column 17, transport and binding proteins; column 18, unknown function. The solid or open bars represent the numbers of genes whose mRNA abundance levels increased or decreased, respectively.

TABLE II
Genes exhibiting the highest induction-fold values at one or more time points following 1 mM potassium chromate exposure

ORF designation	Gene	Gene product function	Mean (K_2CrO_4 /control) ^a at time <i>t</i> (min) ^b			
			5	30	60	90
so3032		Siderophore biosynthesis protein, putative	4.5	10.6	15.6	31.1
so3033		Ferric alcaligin siderophore receptor	3.1	11.8	15.9	21.6
so3062		Hypothetical protein	3.5	10.3	12.9	16.5
so3585		Azoreductase, putative	5.6	60.9	28.2	30.1
so3586		Glyoxalase family protein	3.8	26.4	16.1	13.1
so3587		Hypothetical protein	3.7	17.5	10.4	14.2
so3667 ^c		Conserved hypothetical protein	14.5	25.8	23.7	91.1
so3668 ^c		Conserved hypothetical protein	12.2	14.9	15.9	46.0
so3669	<i>hugA</i>	Heme transport protein	15.5	16.5	20.4	120.0
so3670	<i>tonB1</i>	TonB1 protein	10.3	15.9	25.0	99.0
so3671	<i>exbB1</i>	TonB system transport protein ExbB1	12.8	9.5	15.9	171.8
so3672	<i>exbD1</i>	TonB system transport protein ExbD1	15.2	14.5	22.5	242.3
so3673	<i>hmuT</i>	Hemin ABC transporter, periplasmic hemin-binding protein	11.9	13.9	18.2	40.2
so3674	<i>hmuU</i>	Hemin ABC transporter, permease protein	13.6	14.5	16.9	33.6
so3675	<i>hmuV</i>	Hemin ABC transporter, ATP-binding protein	27.2	17.3	23.4	101.1
so3914		TonB-dependent receptor, putative	6.5	7.5	10.5	44.2

^a Relative gene expression (-fold induction) is presented as the mean ratio of the fluorescence intensity of K_2CrO_4 -exposed cells to control cells. Each gene showed significant differential expression ($p < 0.05$) at least at one time point.

^b Time in minutes at which cells were harvested for RNA isolation following addition of 1 mM K_2CrO_4 to the experimental culture.

^c Genes *so3667* (*hugZ*) and *so3668* (*hugX*) were recently reannotated and predicted to encode heme iron utilization proteins (45).

interval, we observed a large increase in the number of repressed genes involved in energy metabolism.

Real time quantitative RT-PCR was used to provide an independent assessment of gene expression for selected genes across the entire time course of chromate treatment. The six genes (*tonB1*, *tonB2*, *exbB1*, *so2426*, *so3032*, and *so3585*) selected for comparative real time QRT-PCR analysis displayed up-regulated or unchanged expression patterns as identified by microarray analysis. A comparison of gene expression measurements determined by QRT-PCR and microarray analyses indicated that the datasets were highly correlated with an r^2 value of 0.81 ($p < 0.0001$) (see Supplemental Fig. S3).

Induction of Iron Binding and Transport Genes—Of the 910 genes shown to be significantly differentially regulated, we identified a small subgroup comprising 16 genes that exhibited substantially greater expression levels (in some cases >100-fold) compared with the other induced Cr(VI)-responsive genes (Table II). Subgroup IIC (see Supplemental Table S1 and Table II) was dominated by genes encoding products with functions in iron binding and transport: a putative siderophore biosynthesis protein (*so3032*), a ferric alcaligin siderophore receptor (*so3033*), a probable heme transport operon (*hugA-hugX-hugZ*) (44), three TonB1 complex proteins (*tonB1*, *exbB1*, and *exbD1*), and a hemin ABC transporter (*hmuTUV*) (Table II). The expression levels of these affected genes remained induced throughout the time course of acute Cr(VI) exposure. Other genes in the siderophore biosynthesis operon (*so3030-31-32*) and those encoding TonB-dependent receptors (*so1482* and *so1580*), a ferric vibriobactin receptor (*so4516*), and an iron-regulated outer membrane virulence protein (*so4523*) were also up-regulated during the 90-min treatment period but at expression levels much lower in mag-

nitude compared with the genes comprising the putative *tonB1-exbB1-exbD1* operon (Tables II and III).

A number of genes located in different subgroups, whose products are also predicted to be involved in sequestering iron, were induced but at lower levels (e.g. 2–5-fold) compared with those in Subgroup IIC (see Supplemental Table S1 and Table II). These genes included *so3034* (encoding a putative ferric iron reductase protein), *ftn* (encoding ferritin), and *so1158* (encoding a ferritin-like Dps protein). Although the majority of iron binding and transport genes were induced, several genes such as *so1112* and *so1111* (encoding bacterioferritin subunits 1 and 2, respectively) were repressed about 2–5-fold over the time course, and others like *bcp*, which is predicted to encode a bacterioferritin comigratory protein, did not change in response to chromate.

Induction of Detoxification, DNA Damage Repair, and Other Stress-related Genes after Chromate Exposure—The biological basis of chromate-induced toxicity is thought to be the generation of reactive oxygen species (ROS) during enzymatic chromate reduction (for reviews, see Refs. 5 and 7). Cr(V) species are transient intermediates in the flavoenzyme-catalyzed one-electron reduction of chromate whose redox cycling results in the formation of ROS and H_2O_2 generation, which has been shown to be involved in partial chromate reduction (20, 46, 47). Recently the central mechanism of chromium toxicity in *Saccharomyces cerevisiae* was shown to involve oxidative damage to cellular proteins (48). As a strategy for scavenging ROS, bacteria commonly modulate gene expression by inducing genes encoding antioxidant enzymes and proteins. Cr(VI)-stressed *S. oneidensis* MR-1 indicated a 2–5-fold induction of *katG-1* (SO0725, catalase/peroxidase hydroperoxidase), *katB* (SO1070, catalase), and *so4640* (an-

S. oneidensis Chromate Stress Response

TABLE III
Selected genes induced 2-fold or more in response to chromate stress

ORF designation	Gene	Gene product function	Mean (K_2CrO_4 /control) ^a at time <i>t</i> (min) ^b			
			5	30	60	90
DNA replication, recombination, and repair						
so3429	<i>recX</i>	Regulatory protein RecX	1.8	3.9	4.0	4.7
so3430	<i>recA</i>	RecA protein	1.4	4.9	4.9	4.5
so3462	<i>recN</i>	DNA repair protein RecN	2.2	4.2	4.3	4.3
so4603	<i>lexA</i>	LexA repressor	2.1	5.6	5.4	6.4
soa0013	<i>umuD</i>	UmuD protein	1.5	5.1	6.0	5.5
Energy metabolism: electron transport						
so3034		Ferric iron reductase protein, putative	1.9	2.0	4.5	5.1
Hypothetical and conserved hypothetical proteins						
so1188		Conserved hypothetical protein	2.1	3.1	2.8	4.0
so1189		Conserved hypothetical protein	1.8	2.6	2.5	5.7
so1190		Conserved hypothetical protein	1.7	2.6	2.5	5.7
so1450		Conserved hypothetical protein	2.8	5.0	3.2	11.4
so1757		Conserved hypothetical protein	1.3	3.0	7.8	14.7
so3025		Conserved hypothetical protein	1.8	5.1	5.2	7.7
so3724		Hypothetical protein	6.1	7.1	1.3	27.9
so3725		Hypothetical protein	4.9	6.6	1.4	22.7
so4604		Conserved hypothetical protein	2.4	5.9	5.4	6.6
so4605		Hypothetical protein	4.1	7.0	14.0	6.3
so4650		Conserved hypothetical protein	3.8	4.6	3.0	89.2
so4651		Conserved hypothetical protein	5.0	5.5	2.0	45.0
so4656		Hypothetical protein	3.4	6.8	2.8	25.3
Signal transduction						
so2426		DNA-binding response regulator	3.7	3.3	3.5	10.7
Sulfur metabolism						
so3723	<i>cysC</i>	Adenylylsulfate kinase	4.4	6.7	1.6	17.5
so3726	<i>cysN</i>	Sulfate adenylyltransferase, subunit 1	5.0	7.9	1.4	25.5
so3727	<i>cysD</i>	Sulfate adenylyltransferase, subunit 2	4.8	8.0	1.7	24.8
so3736	<i>cysH</i>	Phosphoadenosine-phosphosulfate reductase	3.5	4.6	1.0	15.8
so3737	<i>cysI</i>	Sulfite reductase (NADPH) hemoprotein β -component	3.6	4.7	0.9	13.1
so3738	<i>cysJ</i>	Sulfite reductase (NADPH) flavoprotein α -component	3.8	6.5	1.5	16.3
Transport and binding proteins						
so1482		TonB-dependent receptor, putative	4.3	5.1	3.6	15.2
so1580		TonB-dependent heme receptor	1.9	3.2	4.0	8.4
so2045		Cation efflux family protein	1.9	3.1	2.6	4.6
so3030	<i>alcA</i>	Siderophore biosynthesis protein	2.8	3.0	4.5	9.4
so3031		Siderophore biosynthesis protein, putative	3.6	6.9	10.1	11.4
so3599	<i>cysP</i>	Sulfate ABC transporter, periplasmic sulfate-binding protein	3.6	6.2	1.4	13.3
so4516	<i>viuA</i>	Ferric vibriobactin receptor	5.1	6.8	8.8	22.5
so4523	<i>irgA</i>	Iron-regulated outer membrane virulence protein	2.4	3.6	7.5	10.5
so4652	<i>sbp</i>	Sulfate ABC transporter, periplasmic sulfate-binding protein	4.1	8.4	4.1	41.5
so4654	<i>cysW-2</i>	Sulfate ABC transporter, permease protein	5.1	9.8	2.9	55.0
so4655	<i>cysA-2</i>	Sulfate ABC transporter, ATP-binding protein	3.6	7.1	2.9	25.3
Unknown function/other						
so1114	<i>dinP</i>	DNA damage-inducible protein P	1.9	5.4	5.4	5.0
so1756		Glyoxalase family protein	1.2	2.6	8.1	11.9
so3728	<i>cobA</i>	Uroporphyrin-III C-methyltransferase	4.7	6.5	2.5	18.8

^a Relative gene expression (-fold induction) is presented as the mean ratio of the fluorescence intensity of K_2CrO_4 -exposed cells to control cells. Each gene showed significant differential expression ($p < 0.05$) at least at one time point.

^b Time in minutes at which cells were harvested for RNA isolation following addition of 1 mM K_2CrO_4 to the experimental culture.

toxoidant AhpC/Tsa family protein) at the 60- and 90-min time points (see Supplemental Table S1). Differential expression was not measured for *sodB*, predicted to encode an iron-cofactored superoxide dismutase.

The SOS regulon is a genetic network that enables *Escherichia coli* and related bacteria to maximize their chances of survival when exposed to environmental stresses that dam-

age DNA (for a review, see Ref. 49). Key components in homologous recombination and the SOS pathway of DNA repair were up-regulated at the transcription level in response to Cr(VI) exposure. These up-regulated MR-1 repair genes encoded proteins similar to the LexA (SO4603) repressor, regulatory protein RecX (SO3429), RecA (SO3430), and DNA repair protein RecN (SO3462), which in *E. coli* comprise the

core of the SOS response. Expression of *lexA*, *recX*, *recA*, and *recN* increased substantially after 5 min of acute Cr(VI) exposure and then remained at similar induced levels (~4–6-fold) over the rest of the time course (Table III). Other known SOS-controlled genes, like *dinP* (*so1114*) and plasmid-borne *umuD* (*soa0013*), also displayed expression profiles like that of *recA* (Table III), thus suggesting the induction of an SOS-like pathway of DNA repair and mutagenesis in *S. oneidensis* MR-1 in response to chromate. The *lexA* and *so4604* genes are coupled by overlapping stop and start codons and co-induced in response to UV irradiation, suggesting expression as an operon (35). The downstream *so4605* gene was in the *lexA* and *so4604* expression cluster in response to both UV and chromate stresses, although the putative initiation codon does not overlap with the stop codon of the *so4604* gene.

A putative azoreductase gene (*so3585*) with an annotated function in detoxification, a glyoxalase family gene (*so3586*) of undefined cellular function, and a gene encoding a hypothetical protein (*so3587*) (44) were located within the cluster of highly induced iron-sequestering genes (Table II). Maximal transcriptional induction of *so3585* (61-fold), *so3586* (26-fold), and *so3587* (18-fold) occurred at the 30-min time point followed by continued up-regulation at the 60- and 90-min time points but at lower levels (Table II). These genes have not been shown previously to be involved in the cellular response to chromate stress. *so3585*, *so3586*, and *so3587* are transcribed in the same direction and exhibit co-regulated temporal expression patterns in response to acute Cr(VI) exposure, suggesting that the encoded proteins might function together in a complex. Another gene predicted to encode a glyoxalase family protein (SO1756) exhibited a different temporal expression pattern, characterized by a maximum induction of 12-fold at the 90-min time point (Table III).

Chromate treatment under aerobic growth conditions also resulted in the differential expression of some classic heat shock proteins, chaperones, and proteases, including *groES* (*so0703*), *groEL* (*so0704*), *dnaK* (*so1126*), *ibpA* (*so2277*), *hspG* (*so2016*), *hslUV* (*so4162-63*), *clpB* (*so3577*), *lon* (*so1796*), and *so1987*. These genes exhibited a modest up-regulation (~2–4-fold) early in the transcriptional response to chromate (*i.e.* the 5- and/or 30-min time points), and their increased expression may be indicative of damaged cellular proteins as a result of chromate-induced oxidative stress.

Up-regulated Expression of Sulfate Transport and Sulfur Metabolism Genes—The structural similarity of chromate (CrO_4^{2-}) anions to such biologically important inorganic anions as SO_4^{2-} and PO_4^{3-} most likely constitutes the basis for its active transport across cell membranes via the sulfate transport system (7). Chromate has been shown to be a competitive inhibitor of sulfate transport in *Pseudomonas fluorescens* (26). Based on our array experiments, another subset of MR-1 ORFs that were up-regulated in response to chromate consisted of those genes encoding sulfate ABC transporters (*cysP*, *sbp*, *cysW-2*, and *cysA-2*) and enzymes involved in

activation and subsequent reduction of sulfate to sulfide (*cysC*, *cysDN*, *cysH*, and *cysJ*) (Table III; for a review of sulfur metabolism, see Ref. 50). These genes and predicted operons, along with five hypothetical genes (*so3724*, *so3725*, *so4650*, *so4651*, and *so4656*), displayed a distinctive bimodal pattern of temporal expression with an initial induction peak (~4–10-fold) at the 30-min time interval followed by a marked decrease in transcription and then a second induction (~13–89-fold) at 90 min. The putative serine acetyltransferase gene (*cysE*) was induced ~2-fold at 90 min; however, *cysM* and *cysK*, encoding the two enzymes that catalyze the reaction of *O*-acetylserine with sulfide to yield cysteine, failed to meet our criteria for differential expression. The *so2263–69* genes are immediately downstream of *cysE* and, with the exception of *so2268*, were induced between 2- and 6-fold at one or more time points. In *E. coli*, the B2531–2525 proteins are involved in a sulfur transfer cascade required for the biosynthesis of thiamine, NAD, Fe-S clusters, and thionucleosides (51), and the SO2263–69 proteins showed 65–92% sequence identity between the respective protein counterparts.

Genes Implicated in Regulating the Cellular Response to Chromate—Chromate stress had a greater impact on the expression of genes linked to transcriptional regulatory functions than those with signal transduction functions (Fig. 2). The 90-min time point yielded the most differential expression for transcriptional regulators with 13 and 17 genes being induced and repressed, respectively. These genes included a number of functionally undefined transcriptional regulators from the MerR, TetR, GntR, MarR, and DeoR families (Supplemental Table S1). Genes encoding signal transduction functions were not largely affected by acute chromate treatment: at any one time point only one to three signal transduction genes were induced, and three or four genes were repressed at a single point during the entire exposure period. Most noteworthy was the up-regulation of gene *so2426*, encoding a DNA-binding response regulator of a two-component signaling system. This gene showed a temporal fold induction profile of 3.7 (5 min), 3.3 (30 min), 3.5 (60 min), and 10.7 (90 min) after challenge with 1 mM chromate (Table III). Interestingly this gene was also markedly induced in response to other heavy metal conditions, such as iron overload (39) and nonradioactive strontium stress (37), and may be involved, at least in part, in the coordinate regulation of the cellular response to heavy metal toxicity.

Chromate-mediated Gene Repression—Next to genes encoding hypothetical proteins, energy metabolism showed the most profound temporal changes in terms of the number of genes down-regulated in response to acute chromate exposure (Fig. 2). Although the total number of induced genes (11–19 genes) remained relatively constant over the time course, the number of repressed genes with functions in energy metabolism changed dramatically with 5, 34, 44, and 67 ORFs showing significant decreases in mRNA abundance at the 5-, 30-, 60-, and 90-min time points, respectively. Many

S. oneidensis Chromate Stress Response

TABLE IV
Selected genes down-regulated at least 5-fold at one or more time points in response to chromate stress

ORF designation	Gene	Gene product function	Mean (K ₂ CrO ₄ /control) ^a at time t (min) ^b			
			5	30	60	90
Cellular processes						
<i>so2178</i>	<i>ccpA</i>	Cytochrome c ₅₅₁ peroxidase	1.5	2.2	5.0	2.3
<i>so4053</i>		Methyl-accepting chemotaxis protein	1.1	3.4	6.7	4.3
Central intermediary metabolism						
<i>so0314</i>	<i>speF</i>	Ornithine decarboxylase, inducible	1.3	3.1	11.8	1.3
Energy metabolism						
Amino acids and amines						
<i>so1962</i>		4-Hydroxyphenylpyruvate dioxygenase	1.1	1.8	1.5	7.2
<i>so3774</i>		Proline dehydrogenase/δ-1-pyrroline-5-carboxylate dehydrogenase, putative	3.1	4.1	2.9	7.5
Anaerobic						
<i>so0101</i>	<i>fdnG</i>	Selenium-containing formate dehydrogenase, nitrate inducible, α subunit	1.1	4.3	8.3	3.5
<i>so0102</i>	<i>fdnH</i>	Formate dehydrogenase, nitrate-inducible, iron-sulfur subunit	1.0	3.6	7.3	4.0
<i>so0103</i>	<i>fdnI</i>	Formate dehydrogenase, nitrate-inducible, cytochrome b ₅₅₆ subunit	1.0	3.0	5.4	3.6
<i>so0104</i>	<i>fdhE</i>	FdhE protein	0.9	2.2	5.5	3.0
<i>so0107</i>	<i>fdhD</i>	Formate dehydrogenase accessory protein FdhD	0.8	1.3	6.3	2.9
<i>so0397</i>	<i>fdrC</i>	Fumarate reductase cytochrome b subunit	2.0	3.9	5.1	4.3
<i>so0970</i>		Fumarate reductase flavoprotein subunit precursor	0.5	2.5	8.4	2.6
<i>so4513</i>		Formate dehydrogenase, α subunit	1.4	4.1	12.4	4.5
Electron transport						
<i>so0902</i>	<i>nqrA-1</i>	NADH:ubiquinone oxidoreductase, sodium-translocating, α subunit	1.0	2.6	5.0	5.2
<i>so0903</i>	<i>nqrB-1</i>	NADH:ubiquinone oxidoreductase, sodium-translocating, hydrophobic membrane protein NqrB	0.4	4.4	12.8	5.5
<i>so0904</i>	<i>nqrC-1</i>	NADH:ubiquinone oxidoreductase, sodium-translocating, γ subunit	0.5	6.0	7.6	4.1
<i>so1777</i>	<i>mtrA</i>	Decaheme cytochrome c MtrA	1.0	2.7	6.1	3.4
<i>so1778</i>	<i>omcB</i>	Decaheme cytochrome c	1.0	3.3	5.0	3.3
<i>so1779</i>	<i>omcA</i>	Decaheme cytochrome c	1.2	4.2	8.3	5.4
<i>so3920</i>	<i>hydA</i>	Periplasmic iron hydrogenase, large subunit	1.4	3.2	4.6	5.3
<i>so3921</i>	<i>hydB</i>	Periplasmic iron hydrogenase, small subunit	1.6	3.8	5.2	21.3
<i>so4404</i>		Iron-sulfur cluster-binding protein	0.5	2.3	9.0	5.0
Fermentation						
<i>so2136</i>	<i>adhE</i>	Aldehyde-alcohol dehydrogenase	1.3	7.6	9.5	13.7
Hypothetical and conserved hypothetical proteins						
<i>so0108</i>		Conserved hypothetical protein	0.6	1.1	5.8	3.6
<i>so0109</i>		Conserved hypothetical protein	0.7	1.2	5.9	4.5
<i>so0404</i>		Hypothetical protein	0.9	1.6	5.1	2.5
<i>so0470</i>		Hypothetical protein	1.4	3.3	6.2	2.5
<i>so0595</i>		Hypothetical protein	1.8	4.0	5.0	6.3
<i>so0679</i>		Hypothetical protein	0.7	2.3	2.0	7.9
<i>so0941</i>		Hypothetical protein	0.8	4.0	6.6	3.3
<i>so0975</i>		Hypothetical protein	0.8	5.2	9.6	7.3
<i>so1118</i>		Hypothetical protein	1.3	5.6	7.3	1.3
<i>so1119</i>		Hypothetical protein	0.7	2.0	9.0	2.5
<i>so1250</i>		Conserved hypothetical protein	2.9	5.0	4.6	3.6
<i>so1963</i>		Conserved hypothetical protein	1.2	1.4	1.0	5.9
<i>so2407</i>		Conserved hypothetical protein	0.9	5.3	6.5	6.0
<i>so3542</i>		Conserved hypothetical protein	0.9	2.9	5.2	6.0
<i>so4355</i>		Hypothetical protein	1.3	3.0	5.9	3.5
<i>so4593</i>		Hypothetical protein	0.4	2.2	5.4	2.9
Mobile and extrachromosomal element functions						
<i>soa0061</i>		ParA protein, putative	0.8	1.0	9.9	1.4
Protein synthesis						
<i>so0105</i>	<i>selA</i>	L-Seryl-tRNA selenium transferase	1.0	1.6	6.6	3.2
Purines, pyrimidines, nucleosides, and nucleotides						
<i>so2834</i>	<i>nrdD</i>	Anaerobic ribonucleoside-triphosphate reductase	1.1	2.2	5.8	2.7
Regulatory functions						
<i>so0490</i>		Transcriptional regulator	0.7	3.0	5.6	3.4
<i>so1422</i>		Transcriptional regulator, LysR family	1.2	3.1	8.9	2.9

Downloaded from www.mcponline.org by on November 5, 2007

TABLE IV—continued

ORF designation	Gene	Gene product function	Mean (K_2CrO_4 /control) ^a at time <i>t</i> (min) ^b			
			5	30	60	90
so3059		Formate hydrogenlyase transcriptional activator, putative	1.9	5.5	4.2	4.4
so3297		Transcriptional regulator, LysR family	0.7	4.2	6.2	3.1
so3627		Transcriptional regulator, TetR family	1.0	5.4	10.9	9.0
Signal transduction						
so4155		Sensor histidine kinase	0.9	4.2	6.8	4.3
Transport and binding proteins						
so0028	<i>trkH-2</i>	Potassium uptake protein TrkH	0.7	6.2	8.2	2.9
so0827	<i>lldP</i>	L-Lactate permease	1.2	2.1	5.3	3.3
so2427		TonB-dependent receptor, putative	1.4	3.3	1.8	8.0
so2907		TonB-dependent receptor domain protein	1.9	2.7	1.4	6.5
so3099		Long chain fatty acid transport protein, putative	1.4	2.4	2.9	5.3
so3863	<i>modA</i>	Molybdenum ABC transporter, periplasmic molybdenum-binding protein	1.7	3.8	8.5	8.2
so3864	<i>modB</i>	Molybdenum ABC transporter, permease protein	1.4	3.8	8.3	8.5
Unknown function: enzymes of unknown specificity						
so1911		Oxidoreductase, short chain dehydrogenase/reductase family	1.1	4.8	7.1	3.3
soa0060		Acetyltransferase, GNAT ^c family	1.0	5.5	16.4	2.0

^a Relative gene expression (-fold repression) is presented as the mean ratio of the fluorescence intensity of K_2CrO_4 -exposed cells to control cells. Each gene showed significant differential expression ($p < 0.05$) at least one time point.

^b Time in minutes at which cells were harvested for RNA isolation following addition of 1 mM K_2CrO_4 to the experimental culture.

^c Gcn5-related *N*-acetyltransferase.

of these more highly repressed energy metabolism genes had annotated subrole functions in amino acids and amines (e.g. *so1962* and *so3774*), anaerobic energy metabolism (e.g. *fdnG*, *fdnH*, *fdnI*, *fdhE*, *fdhD*, and *fdrC*), electron transport (e.g. *nqrABC-1*, *mtrA*, *omcA*, *omcB*, and *hydAB*), and fermentation (*adhE*) (Table IV). As shown in Table IV, transcription of genes functioning in cellular processes (e.g. *ccpA*), central intermediary metabolism (*speF*), protein synthesis (*selA*), transcriptional regulation (e.g. *so1422*, *so3297*, and *so3627*), signal transduction (*so4155*), and transport and binding (e.g. *trkH-2* and *modAB*) was significantly repressed under chromate stress conditions.

Proteome Characterization of the Chromate Stress Response—The transcriptome data were compared with and complemented by proteome studies based on mass spectrometry techniques. Cellular fractions from each of the four *S. oneidensis* growth conditions (i.e. Control 1, Control 2, Treatment 1, and Treatment 2) were analyzed in duplicate using 2-D LC-ES-MS/MS with a linear trapping quadrupole mass spectrometer (see “Experimental Procedures” for details). All datasets were searched using SEQUEST (41), filtered and sorted with DTASelect and Contrast (42), and can be accessed directly at compbio.ornl.gov/shewanella_chromium_stress/. The DTASelect files are presented in a viewable html version where every identified spectrum can be viewed by clicking on the spectral number (first column, labeled by filename). The threshold scores used for identification of expressed proteins have been tested rigorously in our laboratory to give a high confidence (see Refs. 43 and 52) and a maximum false-positive rate of 1–2%.

A total of 2,370 of the 4,931 total predicted genes in the *S.*

TABLE V
Proteome analysis of chromate-shocked *S. oneidensis* MR-1

Condition	No. proteins identified	No. proteins identified	Av. sequence coverage ^c
	1 pep ^a	2 pep ^b	%
45-min control	2,610	1,911	37.24
45-min shock	2,644	1,959	37.20
90-min control	2,595	1,892	36.38
90-min shock	2,664	1,992	36.45
Total	2,954	2,370	

^a Total proteins identified with at least one peptide per protein from duplicate runs.

^b Total proteins identified with at least two peptides per protein from duplicate runs.

^c Average sequence coverage per protein at the two-peptide level.

oneidensis MR-1 genome were identified with at least two peptides (Table V), representing 48% of the theoretical proteome. Due to the large number of false positives possible at the one-peptide filter level (52), we present a rigorous analysis of the two-peptide dataset only. High stringency filtering was used in this study, giving a maximum false-positive rate of 1–2%. The reproducibility between duplicate protein analyses on the LTQ was as follows: 78.6% (chromate-shocked) and 78.4% (control) for the 45-min poststress time point and 77.7% (chromate-shocked) and 73.5% (control) for the 90-min time point. This level of reproducibility is necessary for semiquantification. Variation is likely due to low abundance proteins identified with two peptides in one of the analyses and only one peptide in another, thereby being filtered out. Although previous studies using 2-D PAGE and LC-MS/MS

TABLE VI
Functional categories of identified proteins with at least two peptides

Number	Functional category	Observed proteome	Predicted proteome	Percent identified
1	Amino acid biosynthesis	70	91	76.92
2	Biosynthesis of cofactors, prosthetic groups, and carriers	94	121	76.69
3	Cell envelope	121	180	67.22
4	Cellular processes	188	260	72.31
5	Central intermediary metabolism	28	51	54.90
6	DNA metabolism	97	144	67.36
7	Energy metabolism	199	308	64.61
8	Fatty acid and phospholipid metabolism	48	65	73.85
9	Hypothetical proteins	624	2,039	30.60
10	Mobile and extrachromosomal element functions	34	317	10.73
11	Protein fate	137	185	74.05
12	Protein synthesis	131	141	92.91
13	Purines, pyrimidines, nucleosides, and nucleotides	56	62	90.32
14	Regulatory functions	104	199	52.26
15	Signal transduction	39	61	63.93
16	Transcription	49	54	90.74
17	Transport and binding proteins	148	274	54.01
18	Unknown function	203	379	53.56
	Total	2,370	4,931	48.06

have been used for global *S. oneidensis* proteome studies (39, 53, 54), this study represents, to our knowledge, the largest measurement of the *S. oneidensis* proteome published to date.

The entire list of identified proteins with total sequence coverage, functional categories, pI, and molecular weight information is given in Supplemental Table S2. No major biases were found between the pI and molecular weights of the predicted proteome from the genome and the observed proteome (Supplemental Table S2). The identified proteins with their peptide count (number of identified peptides), spectral count (number of MS/MS spectra identified per protein), and percent sequence coverage (total percentage of the protein sequence covered by tryptic peptides) for the different growth conditions and individual analyses can be found in Supplemental Table S3.

Proteins identified at the two-peptide level were grouped according to the functional categories assigned by The Institute for Genomic Research annotation (Ref. 44; www.tigr.org, Comprehensive Microbial Resource) (Table VI). Proteins with assigned functions in amino acid biosynthesis, cellular processes, protein fate, protein synthesis, nucleotide metabolism, and transcription were found with greater than 70% identified. More than 90% of the proteins comprising the functional classes of protein synthesis, nucleotide metabolism, and transcription were identified, representing an almost complete characterization of these categories at the proteome level. Proteins generally thought to be of lower abundance, such as those with assigned functions in signal transduction and transcriptional regulation, were identified at levels of 64 and 52%, respectively, of the total number of proteins per category. A total of 624 of the 2,039 predicted hypothetical proteins were identified. Of the 624 proteins in this functional category, 209 were annotated as hypothetical proteins,

and 415 were annotated as conserved hypothetical proteins. This represents one of the largest identifications of hypothetical protein expression for a microbial proteome to date.

Comparison of Transcriptome and Proteome Data—Although absolute quantification at the global proteome level was not feasible, semiquantification of differentially expressed proteins between the chromate-treated and control samples could be accomplished by using a combination of percent sequence coverage, number of unique peptides, and spectral count from the mass spectra (39, 43, 55) (see “Experimental Procedures” for details). Other methods for relative quantification, such as ICAT, were considered before the method used here was selected. ICAT labels the cysteine residues of a protein, and in *S. oneidensis* greater than 50% of the predicted proteins have two or fewer cysteine residues present. Moreover almost 20% of the predicted proteome does not contain any cysteine residues. This method would not detect almost 70% of the predicted proteome confidently; thus ICAT was not deemed appropriate for this study.

Comparisons were made between the transcriptome and proteome data to determine the relationship between gene and protein expression. Both up- and down-regulated proteins were measured by comparing the chromate-shocked cell samples to their respective control samples. Using the semiquantitative criteria discussed above, we identified 78 proteins (Supplemental Table S4) as being differentially expressed in response to chromate (Tables VII and VIII and Supplemental Table S4). Supplemental Table S4 divides the proteins identified at 45 min postshock from the proteins identified at 90 min postshock. We propose that reproducibility of at least 70% between replicate analyses at the protein level is necessary for a successful determination of differentially expressed proteins where a protein must be detected in

TABLE VII
Up-regulated proteins identified in the 90-min chromate-shocked sample

Protein	Transcriptome	Control 1	Control 2	Treatment 1	Treatment 2	Category	Description
SO0343	No change ^a	20.8	18.3	43.3	45.7	7	Aconitate hydratase 1 (<i>acnA</i>)
SO0423	Induced ^b	11.2	0.0	43.6	39.2	14	Pyruvate dehydrogenase complex repressor (<i>pdhR</i>)
SO0798	Induced	0.0	0.0	24.7	21.7	9	Conserved hypothetical protein
SO0934	No change	12.2	55.5	87.8	76.3	9	Conserved hypothetical protein
SO1045	No change	0.0	0.0	22.3	24.5	9	Hypothetical protein
SO1114 ^c	Induced	0.0	0.0	28.3	55.2	18	DNA damage-inducible protein P (<i>dinP</i>)
SO1178	No change	11.7	11.3	45.7	41.6	17	Magnesium and cobalt efflux protein CorC (<i>corC</i>)
SO1190 ^c	Induced	39.0	20.2	55.5	51.8	9	Conserved hypothetical protein
SO1482 ^c	Induced	30.2	28.8	82.7	80.5	17	TonB-dependent receptor, putative
SO1576	No change	20.7	0.0	39.2	44.6	4	Glutathione S-transferase family protein
SO1580 ^c	Induced	5.0	14.0	29.0	45.3	17	TonB-dependent heme receptor
SO1755	Induced	22.3	10.6	34.6	49.6	7	Phosphoglucomutase/phosphomannomutase family protein
SO2290	No change	24.9	17.4	49.8	48.0	18	Rhodanese domain protein
SO2426 ^c	Induced	0.0	0.0	37.1	48.1	15	DNA-binding response regulator
SO2577	No change	6.3	22.3	41.3	48.7	4	Septum site-determining protein MinD (<i>minD</i>)
SO2912 ^c	Induced	38.3	25.9	64.7	55.1	7	Formate acetyltransferase (<i>pfIB</i>)
SO2915	Induced	15.5	12.3	49.4	43.6	5	Acetate kinase (<i>ackA</i>)
SO3030 ^c	Induced	12.9	0.0	62.4	66.1	17	Siderophore biosynthesis protein (<i>alcA</i>)
SO3032 ^c	Induced	5.7	0.0	31.4	32.3	17	Siderophore biosynthesis protein, putative
SO3033 ^c	Induced	12.0	6.7	57.6	57.3	17	Ferric alcaligin siderophore receptor
SO3061	Induced	6.1	3.1	31.3	37.9	6	DNA topoisomerase III (<i>topB</i>)
SO3407	Induced	9.3	8.8	24.7	19.1	9	Conserved hypothetical protein
SO3462 ^c	Induced	0.0	6.0	35.1	34.1	6	DNA repair protein RecN (<i>recN</i>)
SO3585 ^c	Induced	0.0	0.0	20.1	23.0	4	Azoreductase, putative
SO3586 ^c	Induced	0.0	0.0	60.1	20.3	18	Glyoxalase family protein
SO3599	Induced	12.8	18.5	68.7	64.8	17	Sulfate ABC transporter, periplasmic protein (<i>cysP</i>)
SO3667 ^c	Induced	0.0	0.0	91.9	96.8	9	Conserved hypothetical protein ^d
SO3669 ^c	Induced	9.3	11.6	71.6	77.9	17	Heme transport protein (<i>hugA</i>)
SO3670 ^c	Induced	0.0	0.0	13.5	18.6	17	TonB1 protein (<i>tonB1</i>)
SO3671	Induced	0.0	0.0	20.4	26.5	17	TonB system transport protein ExbB1 (<i>exbB1</i>)
SO3673 ^c	Induced	0.0	0.0	63.1	61.2	17	Hemin ABC transporter, periplasmic protein (<i>hmuT</i>)
SO3675 ^c	Induced	0.0	0.0	72.9	59.0	17	Hemin ABC transporter, ATP-binding protein (<i>hmuV</i>)
SO3723	Induced	0.0	0.0	50.2	29.8	5	Adenylylsulfate kinase (<i>cysC</i>)
SO3726	Induced	22.1	7.8	49.7	49.3	5	Sulfate adenylyltransferase, subunit 1 (<i>cysM</i>)
SO3727	Induced	38.7	20.2	68.5	68.5	5	Sulfate adenylyltransferase, subunit 2 (<i>cysD</i>)
SO3737	Induced	30.8	22.1	62.1	73.3	5	Sulfite reductase (NADPH) hemoprotein (<i>cysI</i>)
SO3738	Induced	5.9	0.0	30.8	27.3	5	Sulfite reductase (NADPH) flavoprotein (<i>cysJ</i>)
SO3907	No change	0.0	0.0	48.1	60.0	9	Conserved hypothetical protein
SO3913 ^c	Induced	0.0	0.0	27.2	32.6	9	Conserved hypothetical protein
SO3914 ^c	Induced	18.5	15.8	68.1	67.8	17	TonB-dependent receptor, putative
SO4077	Induced	14.5	14.0	36.7	37.1	17	TonB-dependent receptor, putative
SO4516	Induced	0.0	8.8	37.7	32.6	17	Ferric vibriobactin receptor (<i>viuA</i>)
SO4523	Induced	39.4	50.5	70.8	74.4	17	Iron-regulated outer membrane virulence protein (<i>irgA</i>)
SO4651 ^c	Induced	0.0	0.0	41.4	77.6	9	Conserved hypothetical protein
SO4652 ^c	Induced	0.0	0.0	46.6	62.0	17	Sulfate ABC transporter, periplasmic protein (<i>sbp</i>)
SO4655 ^c	Induced	0.0	0.0	54.5	55.1	17	Sulfate ABC transporter, ATP-binding protein (<i>cysA-2</i>)
SO4743	Induced	50.9	49.9	71.7	67.7	17	TonB-dependent receptor, putative
SOA0042	No change	0.0	0.0	46.9	46.3	9	Hypothetical protein

^a No change in expression at the 90-min time point in the microarray analysis. No change defines a gene that was found to not have an induction or repression of expression at any time point on the microarray.

^b Induced defines a gene that exhibited at least 2-fold induction at the 90-min time point.

^c Proteins also found to be up-regulated in the 45-min chromate exposure samples.

^d The functional annotation of SO3667 was revised recently to a heme iron utilization protein, HugZ (45).

both of the replicate analyses to be included as a candidate for semiquantification.

For the 45-min chromate treatment analysis, a total of 24 proteins were found to be up-regulated with six additional

proteins being down-regulated relative to the control sample (Supplemental Table S4). The genes for 23 of these 24 up-regulated proteins showed corresponding induction levels at the 30- and 60-min time points based on microarray hybrid-

TABLE VIII
Down-regulated proteins identified in the 90-min chromate-shocked samples

Protein	Transcriptome	Control 1	Control 2	Treatment 1	Treatment 2	Category	Description
SO0398	Repressed ^a	42.4	18.1	0.0	4.6	7	Fumarate reductase flavoprotein subunit (<i>frdA</i>)
SO0404	Repressed	78.8	77.9	55.4	57.2	9	Hypothetical protein
SO0548	Repressed	70.0	76.7	47.8	51.1	6	DNA-binding protein, HU family
SO0847	Induced	45.9	28.7	0.0	0.0	7	Iron-sulfur cluster-binding protein NapG (<i>napG</i>)
SO0848 ^b	Induced ^c	73.2	52.9	43.8	46.1	7	Periplasmic nitrate reductase (<i>napA</i>)
SO0902	Repressed	49.8	37.5	26.5	18.4	7	NADH:ubiquinone oxidoreductase (<i>nqrA-1</i>)
SO0970	Repressed	59.9	57.4	34.7	34.9	7	Fumarate reductase flavoprotein subunit precursor
SO1111	Repressed	75.8	70.1	35.7	42.7	17	Bacterioferritin subunit 2 (<i>bfr2</i>)
SO1405	No change ^d	40.1	31.4	11.1	0.0	18	Transglutaminase family protein
SO1429	No change	42.8	26.8	0.0	0.0	7	Anaerobic dimethyl sulfoxide reductase, A (<i>dmaA-1</i>)
SO1430	No change	31.2	36.2	0.0	0.0	7	Anaerobic dimethyl sulfoxide reductase, B (<i>dmsB-1</i>)
SO1490	Repressed	67.3	70.2	27.2	39.8	7	Alcohol dehydrogenase II (<i>adhB</i>)
SO1518	Repressed	80.4	81.5	48.1	52.4	9	Conserved hypothetical protein
SO1776	Repressed	48.5	41.9	25.7	31.0	3	Outer membrane protein precursor MtrB (<i>mtrB</i>)
SO1777	Repressed	8.7	6.9	0.0	0.0	7	Decaheme cytochrome c MtrA (<i>mtrA</i>)
SO1778	Repressed	43.4	55.1	25.0	25.2	7	Decaheme cytochrome c (<i>omcB</i>)
SO1779	Repressed	51.8	53.5	26.7	29.9	7	Decaheme cytochrome c (<i>omcA</i>)
SO2469	Repressed	22.1	24.7	10.0	12.1	18	Conserved hypothetical protein
SO2490	Repressed	51.8	66.9	33.5	28.9	14	Transcriptional regulator, RpiR family
SO2929 ^b	Repressed	73.8	73.0	36.3	40.0	9	Hypothetical protein
SO3538 ^b	Repressed	46.9	34.7	0.0	0.0	14	transcriptional regulator HlyU (<i>hlyU</i>)
SO3565	Repressed	72.0	59.9	36.8	39.6	13	2,3-Cyclic-nucleotide 2-phosphodiesterase (<i>cpdB</i>)
SO3920	Repressed	21.7	27.6	0.0	0.0	7	Periplasmic iron hydrogenase, large subunit (<i>hydA</i>)
SO3967	No change	71.6	56.4	23.0	24.5	17	Molybdenum ABC transporter, periplasmic
SO4513 ^b	No change	44.3	36.2	3.3	3.5	7	Formate dehydrogenase, α subunit
SO4561	No change	37.7	47.4	0.0	0.0	9	Conserved hypothetical protein

^a Repressed defines a gene that exhibited at least 2-fold repression at the 90-min time point.

^b Proteins found to be down-regulated in both the 45- and 90-min chromate exposure experiments.

^c Induced defines a gene that exhibited at least 2-fold induction at the 90-min time point.

^d No change in expression at the 90-min time point in the microarray analysis. No change defines a gene that was found to not have an induction or repression of expression at any time point on the microarray.

ization. A putative formate acetyltransferase (encoded by *pflB*), which was identified as being up-regulated at the protein level, was found to be induced at the transcript level at the 30-min treatment time but repressed at the 60-min time point. The subset of proteins identified as up-regulated were dominated by species (12 total) assigned to the functional category of transport and binding proteins and included TonB-dependent receptors, siderophore biosynthesis proteins, heme transport proteins, and TonB1. Proteins classified as hypothetical were also dominant with a total of six conserved hypothetical proteins identified as up-regulated.

For the six proteins down-regulated in the 45-min shocked sample relative to the control condition, five were found to be repressed at the mRNA level by microarray analysis, and the other protein, a hypothetical protein (SOA0141), revealed no change at the transcript level. Proteins that were measured as being down-regulated in the 45-min chromate-shocked samples consisted of three hypothetical proteins (SO1124, SO2929, and SOA0141), a periplasmic nitrate reductase (NapA), a transcriptional regulator (HlyU), and the α subunit of formate dehydrogenase (SO4513).

Proteomic analysis of the 90-min chromate treatment sam-

ples revealed 48 up-regulated proteins and 26 down-regulated proteins relative to the control sample (Supplemental Table S4 and Tables VII and VIII). After 90 min of chromate exposure, 39 of the 48 proteins up-regulated under Cr(VI) conditions also were induced at the transcript level as identified by microarray analysis. Nine of the up-regulated proteins (AcnA, SO0934, SO1045, CorC, SO1576, SO2290, MinD, SO3907, and SOA0042) revealed no significant change ($p < 0.05$) in expression at the transcription level, and two of the proteins (AcnA and SO2290) expressed at higher abundance levels under chromate stress conditions did not exhibit a change in their mRNA expression levels at the 90-min time point but did at earlier time points (5, 30, and 60 min). Of the 48 up-regulated proteins, 19 proteins were from the transport and binding category, six proteins were from central intermediary metabolism, and 10 were annotated as hypothetical proteins. All of the transport and binding proteins identified as up-regulated in the 45-min chromate-shocked samples were also identified as up-regulated in the 90-min samples, whereas only four of the six conserved hypothetical proteins showed up-regulation at both postexposure time points.

Eighteen of 26 proteins down-regulated 90 min after chro-

mate addition were also repressed at the transcript level. Of the remaining down-regulated proteins, five showed no change at the mRNA level, one protein of which was found to exhibit no mRNA change at the 90-min time point. Two down-regulated proteins (NapG and NapA) were found to be induced at the transcript level. Four of the six proteins down-regulated at the 45-min time point were also repressed at 90 min. The transcriptome data revealed an increase in the number of down-regulated energy metabolism genes over time in response to chromate. This trend was also reflected in the proteomic data in which 13 proteins with functions in energy metabolism were identified as repressed at the 90-min time point relative to the 45-min interval.

Differences between the transcriptomic and proteomic responses of *S. oneidensis* to chromate shock are due to the stringency of filtering used in the proteome study and inherent measurement differences between microarray *versus* proteome technology. Supplemental Table S5 demonstrates the correlation of the identified and/or differentially expressed proteins to the top 100 mRNAs induced at each time point. The list is composed of a total of 194 mRNAs, which is a concatenated list representing the top 100 mRNAs at each time point (initial list was 400 genes in total before removal of redundant genes). A total of 67% of the genes in Supplemental Table S5 did not meet the differential criteria at the protein level where 45% were not identified by mass spectrometry and another 22% were not considered differentially expressed. The 67% of genes found not to meet differential expression criteria corresponds to 130 genes of 194, which is comparative in percentage to the total global analysis.

DISCUSSION

A global analysis of the *S. oneidensis* temporal response to a toxic concentration (1 mM) of chromate was performed by integrating whole-genome microarray hybridization and 2-D HPLC-MS/MS techniques. This study provides the first comprehensive molecular description of the response of a dissimilatory metal-reducing bacterium to an acute challenge of toxic chromate, a serious anthropogenic pollutant found in diverse environmental settings. Five major features characterized the molecular dynamics underlying the *S. oneidensis* response to acute chromate stress: 1) the induction of genes/proteins involved in iron transport and sulfur assimilation; 2) co-regulated induction of the gene cluster *so3585*, *so3586*, and *so3587*; 3) up-regulation of DNA repair genes and their encoded protein products; 4) differential expression of a large number of hypothetical genes/proteins; and 5) a dramatic increase in the number of down-regulated energy metabolism genes and proteins over time.

As revealed by transcriptome and proteome analyses, a major feature of the molecular response of *S. oneidensis* MR-1 to acute chromate challenge was the differential regulation of the TonB1-ExbB1-ExbD1 complex, an integral inner membrane system for iron transport, as well as other genes

involved in exogenous iron acquisition. Genes that were highly induced based on time series microarray experiments (Table II) and were identified as up-regulated proteins at the 45- and/or 90-min chromate treatment conditions (Table VII) included two putative siderophore biosynthesis proteins (AlcA and SO3032), a ferric alcaligin siderophore receptor (SO3033), HugA heme transport protein (SO3669), TonB1 (SO3670), a putative TonB-dependent receptor (SO3914), a TonB-dependent heme receptor (SO1580), ViuA (SO4516), and HmuT (SO3673) and HmuV (SO3675) of the hemin ABC transporter. Wang and Newton (56) demonstrated that mutants harboring a deletion of the *tonB-trp* region of the *E. coli* chromosome were sensitive to chromic ion (Cr^{3+}) due to defective iron transport systems, and residual iron uptake by these strains was shown to be inhibited by chromic ion. Regulation of iron homeostasis is primarily carried out by the Fur protein (for a review, see Ref. 57). It has been suggested previously that iron uptake regulation may not be the only function of Fur but that it may also serve to sequester iron to prevent the generation of highly reactive hydroxyl radicals via Fenton reactions (58). The putative MR-1 ferritin genes, but not bacterioferritin genes, were induced in response to chromate, and these respective iron storage proteins have been suggested to have roles in short term iron flux and long term iron storage in *E. coli* (59).

In addition to iron transport genes, our global analyses demonstrated that CysP, CysC, CysD, CysN, CysI, CysJ, Sbp, and CysA-2 are up-regulated at both the mRNA and protein levels in response to chromate treatment (Tables III and VII). The enhanced expression of genes encoding proteins involved in sulfate transport and assimilatory sulfate reduction suggests the possibility of chromate-induced sulfur limitation in *S. oneidensis*, perhaps through competitive inhibition of sulfate uptake by chromate, as has been shown previously (26, 30). Partial reduction of Cr(VI) to Cr(V) produces ROS (6, 7, 20), leading to chromate-mediated oxidative stress. Researchers working with a number of different bacteria have observed induction of genes involved in sulfur and iron homeostasis following different oxidative stresses (35, 60–62). A variety of explanations have been proposed including disruption of intracellular redox cycling leading to insufficient sulfite reduction, a reduction in cysteine biosynthesis correlated with cell envelope damage and subsequent leakage of sulfide (63), and increased demand for low molecular weight protective thiol-containing compounds such as glutathione (64). Alternatively induction of genes involved in sulfur metabolism and iron sequestration might represent an adaptive response to sulfur and iron limitation in MR-1 following chromate exposure.

One of the potentially interesting findings to emerge from this integrated global investigation was the co-regulated expression of a cluster of three genes (*so3585*, *so3586*, and *so3587*) at both the mRNA and protein levels. All three genes are transcribed in the same direction on the MR-1 chromo-

some and show a similar transcriptional profile in response to chromate with the peak in up-regulated expression occurring at the 30-min time point (Table II). The proteins encoded by two of these genes (*so3585* and *so3586*) were detected in the chromate-treated samples only (Table VII), suggesting that expression of SO3585 and SO3586 was differentially regulated in response to chromate stress conditions. By contrast, hypothetical protein SO3587 was found in both the control and chromate-shocked samples at the two-peptide level (Supplemental Table S3) even though the gene encoding this protein was shown to be up-regulated over the entire time course in response to chromate stress. In addition, SO3587 was found only in the membrane fractions, and a hydrophobicity plot analysis using the computer program SOSUI (65) identified a putative transmembrane domain (IGIALIFADVSLYLAYFFVGLGV) in SO3587. SO3585 and SO3586 were detected in both the soluble and membrane fractions. Based on their proximity in genome location and co-regulated expression profile within the context of chromate stress, we predict that SO3585, SO3586, and SO3587 function together as a protein complex associated with the cell membrane and play an important role in the response of the cell to chromate toxicity.

S. oneidensis SO3585 and SO3586 are annotated as a putative azoreductase and glyoxalase family protein, respectively (44). Glyoxalase systems are known to serve as key detoxification routes for preventing the intracellular accumulation of methylglyoxal, a natural metabolite with toxic electrophilic properties (for a review, see Ref. 66). Azoreductases are responsible for the reductive cleavage of azo dyes, synthetic organic colorants used extensively in the textile, food, and cosmetics industries. Synthetic azo dyes are not readily reduced under aerobic conditions and are considered pollutants. Protein database searches using BLAST Version 2.2.12 (67) with the derived SO3585 primary sequence revealed ~28% sequence identity with *P. putida* ChrR and *E. coli* YieF, two soluble flavoproteins that have been demonstrated to exhibit chromate reductase activity (18, 46, 68). Regions of conservation in the derived amino acid sequence of SO3585 included the characteristic signature, LFVTP⁶EYNX⁶LKNAIDX²S (conserved residues in SO3585 are underlined), of the NADH_{dh2} family of NAD(P)H oxidoreductases (Ref. 46; results not shown). Recently further investigation demonstrated that the *P. putida* ChrR functions as a quinone reductase and minimizes oxidative stress induced by intracellular H₂O₂, which is generated during the course of chromate reduction (69). An MR-1 strain carrying an in-frame deletion mutation in the *so3585* locus has been created, and future studies will characterize it to gain insight into the functional role of SO3585 and to assess the importance of azoreductase in the *S. oneidensis* response to chromate.

Another primary feature of the molecular response to chromate was the stimulation of genes whose protein products are involved in DNA repair mechanisms, thus indicating a contri-

bution of genotoxic damage to chromate toxicity in *S. oneidensis*. Genes with functions linked to DNA damage, recombination, and repair (*dinP*, *recX*, *recA*, *recN*, *lexA*, and *umuD*) exhibited similar temporal expression profiles when cells were challenged with 1 mM chromate: the transcript levels for all six genes increased only slightly (1.5–2-fold) early in the treatment followed by induction plateaus of 4–6-fold from the 30-min time point onward (Table III). Only two of these genes (*dinP* and *recN*) showed corresponding increases in the abundance levels of their expressed proteins at both the 45- and 90-min time points following chromate treatment (Table VII); RecA and LexA were also identified at the protein level but did not show differential expression. Members of the *E. coli* SOS regulon, which includes genes encoding the DNA damage-inducible (Din) proteins, are controlled by the RecA coprotease activity and LexA repressor and are transcriptionally induced following DNA damage (for a review, see Ref. 49). The induction of homologs for such known SOS-controlled genes as *recA*, *lexA*, *recN*, and *umuD* suggests chromate-induced DNA damage in *S. oneidensis* and subsequent RecA activation and LexA cleavage under the selected conditions. Qiu *et al.* (35) similarly observed induction of the MR-1 SOS response and active detoxification mechanisms following oxidative damage caused by UV radiation. The precise mechanism underlying chromate-induced DNA damage in *S. oneidensis* has not been determined. However, oxidative DNA damage, triggered by Cr(V) complexes reacting with H₂O₂ to generate hydroxyl radicals, is considered the basis of chromium genotoxicity (7, 22–24) and likely produces an SOS-like response in MR-1. The study by Qiu *et al.* (35) and this investigation revealed two genes (*so4604* and *so4605*) downstream of the *lexA* gene that were induced following different oxidative stress conditions, and their expression profiles clustered together with *lexA*. However, further studies are required to determine whether these genes are directly involved in the MR-1 SOS response.

In addition to members comprising a potential SOS regulon in *S. oneidensis*, we demonstrated the induction of *topB* (encodes a DNA topoisomerase III) at both the mRNA and protein levels. Topoisomerase III was initially described as exhibiting superhelical DNA relaxing activity (70). A recent study by Nurse *et al.* (71) demonstrated that topoisomerase III can function as the principal cellular decatenase, capable of uncoupling replicating daughter chromosomes *in vivo*. Microarray analysis revealed a temporal expression pattern for *S. oneidensis topB* resembling that of *recA* and other DNA damage-inducible genes (Supplemental Table S1). A chromate-dependent increase in TopB abundance levels was observed only at the 90-min time point (Table VII). Trivalent chromium has been reported to cause DNA damage and inhibit type II topoisomerase-mediated DNA relaxation activity in bacterial cells (72). Although we did not detect chromate reduction during the treatment period (Supplemental Fig. S1), our transcriptome and proteome data suggest that chromate

has an impact on DNA topology leading to adjustments in the expression levels for cellular topoisomerases.

The large portion of genes with unassigned cellular functions among Cr(VI)-induced or Cr(VI)-repressed genes reveals how much of the molecular response of *S. oneidensis* to chromate toxicity remains to be explored. At each time point after chromate addition, ~39–50% of the total number of induced genes and 31–47% of the total number of repressed genes were functionally classified as hypothetical or conserved hypothetical proteins. Fifty percent of the genes up-regulated at the 90-min interval in response to chromate were functionally unknown, whereas poorly characterized genes constituted 31% of the total number of down-regulated genes at that time point. Nine proteins (SO0798, SO0934, SO1045, SO1190, SO3667, SO3907, SO3913, SO4651, and SOA0042) annotated as hypothetical or conserved hypothetical met our criteria of significance for differential expression and were identified as being up-regulated in response to chromate exposure at the 45- and/or 90-min time points (Table VII). For four of these proteins (SO0934, SO1045, SO3907, and SOA0042), we observed no significant change in expression at the mRNA level, suggesting post-transcriptional regulation of these proteins in response to chromate. Our integrated transcriptome and proteome study implicates these differentially regulated proteins of unknown function in the initial response of MR-1 to toxic chromate, thus revealing gene candidates for future functional analysis.

A recent study by Kolker *et al.* (45) analyzed expression for a subset of 538 hypothetical proteins that were confidently identified in *S. oneidensis* MR-1 as a result of large scale microarray and proteomic analyses of cell samples generated under different growth conditions. A total of 788 hypothetical proteins have been identified based on the study by Kolker *et al.* (45) and the present study: 368 of these functionally undefined proteins were found in both studies, 170 were found only by Kolker *et al.* (45), and 256 were found only in this study (Supplemental Table S6). The 368 hypothetical proteins identified independently by both studies should be considered as expressed proteins, and their annotations should be changed to unknown or conserved unknown (43). Most of these proteins were found under all growth conditions and identified in most of the replicates. Differences between the datasets revealed by this proteomic study and the one reported by Kolker *et al.* (45) are likely due to differences in the growth conditions used.

Finally the *S. oneidensis* response to chromate was distinguished by a time-dependent and dramatic increase in the number of down-regulated genes with functions in energy metabolism (Fig. 2). With the exception of the hypothetical protein category, chromate had the greatest impact on energy metabolism in terms of the number of repressed genes: five (5 min), 34 (30 min), 44 (60 min), and 67 (90 min). Genes with annotated functions in anaerobic energy metabolism and electron transport were particularly affected by chromate

treatment with ORFs encoding the formate dehydrogenase subunits (*fdnGHI*), NADH:ubiquinone oxidoreductase subunits (*nqrABC-1*), MtrA, OmcA, OmcB, and periplasmic iron hydrogenase subunits (*hydAB*) showing some of the highest repression -fold values at the 60- or 90-min time point (Table IV). Within this subset of genes, proteins NqrA-1, MtrA, OmcA, OmcB, and HydA were also detected at decreased abundance levels (Table VIII). In addition, MS-based proteomics revealed potential instances of post-transcriptional regulation of gene expression in response to chromate stress. For example, proteome analysis indicated complete repression of the anaerobic dimethyl sulfoxide reductase subunits A (SO1429) and B (SO1430) under chromate treatment conditions, whereas no significant change in expression at the transcript level was observed for *dmaA-1* and *dmsB-1* (Table VIII).

In summary, we used integrated transcriptome and proteome analyses to reveal a global view of the response of the metal-reducing bacterium *S. oneidensis* MR-1 to the challenge of acute chromate stress. The molecular response of *S. oneidensis* to chromate shock elicited a distinctively different transcriptional profile compared with Cr(VI) reduction by MR-1 in a study published recently (73). Approximately 20% of the genes up-regulated during chromate reduction encode putative cytochromes, cytochrome synthesis proteins, or noncytochrome reductases (which were repressed or not differentially expressed in the present study), consistent with cells being potentially limited for iron under Cr(VI)-shocked conditions. The chromate shock response of *S. oneidensis* requires a combination of different regulatory networks that involve genes with annotated functions in oxidative stress protection, detoxification, protein stress protection, iron and sulfur acquisition, and DNA repair mechanisms.

Acknowledgments—We thank Liyou Wu, Xueduan Liu, and Tingfen Yan for the construction of whole-genome microarrays for *S. oneidensis* MR-1 and Xiu-Feng Wan for hydrophobicity plot analysis.

* This work was supported in part by the United States Department of Energy, Office of Science, Biological and Environmental Research programs. Oak Ridge National Laboratory is managed by University of Tennessee-Battelle LLC for the Department of Energy under Contract DOE-AC05-00OR22725. The costs of publication of this article were defrayed in part by the payment of page charges. This article must therefore be hereby marked “advertisement” in accordance with 18 U.S.C. Section 1734 solely to indicate this fact.

§ The on-line version of this article (available at <http://www.mcponline.org>) contains supplemental material.

§ Both authors contributed equally to this work.

** Received support from the University of Tennessee (Knoxville)-Oak Ridge National Laboratory Graduate School of Genome Science and Technology.

§§ To whom correspondence for mass spectrometry and proteomics should be addressed: Chemical Sciences Division, Oak Ridge National Laboratory, P. O. Box 2008 MS-6131, Oak Ridge, TN 37831-6131. Tel.: 865-574-4968; Fax: 865-576-8559; E-mail: hettichrl@ornl.gov.

||| To whom correspondence for microarray analysis and *Shewanella* growth should be addressed: Dept. of Biological Sciences,

Purdue University, 1-118 Lilly Hall of Life Sciences, 915 West State St., West Lafayette, IN 47907-2054. Tel.: 765-496-8301; Fax: 765-494-0876; E-mail: dthomps@purdue.edu.

REFERENCES

- James, B. R. (1996) The challenge of remediating chromium-contaminated soil. *Environ. Sci. Technol.* **30**, A248–A251
- Langard, S. (1980) *Metals in the Environment*, pp. 111–132, Academy Press Inc., New York
- Riley, R. G., Zachara, J. M., and Wobber, F. J. (1992) *Chemical Contaminants on DOE Lands and Selection of Contaminant Mixtures for Subsurface Science Research*, Report DOE/ER-0547T, United States Department of Energy, Washington, D. C.
- Katz, S. A., and Salem, H. (1993) The toxicology of chromium with respect to its chemical speciation: a review. *J. Appl. Toxicol.* **13**, 217–224
- Klein, C., Snow, E., and Frenkel, K. (1998) *Molecular Biology of Free Radicals in Human Diseases*, pp. 79–137, Academic Press, New York
- Singh, J., Carlisle, D. L., Pritchard, D. E., and Patierno, S. R. (1998) Chromium-induced genotoxicity and apoptosis: relationship to chromium carcinogenesis. *Oncol. Rep.* **5**, 1307–1318
- Cervantes, C., Campos-García, J., Devars, S., Gutiérrez-Corona, F., Loza-Tavera, H., Torres-Guzmán, J. C., and Moreno-Sánchez, R. (2001) Interactions of chromium with microorganisms and plants. *FEMS Microbiol. Rev.* **25**, 335–347
- Schmieman, E. A., Yonge, D. R., Rege, M. A., Petersen, J. N., Turick, C. E., and Apel, W. A. (1998) Comparative kinetics of bacterial reduction of chromium. *J. Environ. Eng.* **124**, 449–455
- Turick, C. E., Apel, W. A., and Carmiol, N. S. (1996) Isolation of hexavalent chromium-reducing anaerobes from hexavalent-chromium contaminated and noncontaminated environments. *Appl. Microbiol. Biotechnol.* **44**, 683–688
- Wang, Y. T., and Shen, H. (1995) Bacterial reduction of hexavalent chromium. *J. Ind. Microbiol.* **14**, 159–163
- Daulton, T. L., Little, B. J., Lowe, K., and Jones-Meehan, J. (2002) Electron energy loss spectroscopy techniques for the study of microbial chromium(VI) reduction. *J. Microbiol. Methods* **50**, 39–54
- Myers, C. R., Carstens, B. P., Antholine, W. E., and Myers, J. M. (2000) Chromium(VI) reductase activity is associated with the cytoplasmic membrane of anaerobically grown *Shewanella putrefaciens* MR-1. *J. Appl. Microbiol.* **88**, 98–106
- Viamajala, S., Peyton, B. M., Apel, W. A., and Petersen, J. N. (2002) Chromate/nitrite interactions in *Shewanella oneidensis* MR-1: evidence for multiple hexavalent chromium [Cr(VI)] reduction mechanisms dependent on physiological growth conditions. *Biotechnol. Bioeng.* **78**, 770–778
- Caccavo, F., Ramsing, N. B., and Costerton, J. W. (1996) Morphological and metabolic responses to starvation by the dissimilatory metal-reducing bacterium *Shewanella alga* BrY. *Appl. Environ. Microbiol.* **62**, 4678–4682
- Nyman, J. L., Caccavo, F., Cunningham, A. B., and Gerlach, R. (2002) Biogeochemical elimination of chromium(VI) from contaminated water. *Biorem. J.* **6**, 39–55
- Wielinga, B., Mizuba, M. M., Hansel, C. M., and Fendorf, S. (2001) Iron promoted reduction of chromate by dissimilatory iron-reducing bacteria. *Environ. Sci. Technol.* **35**, 522–527
- Wang, P., Mori, T., Toda, K., and Ohtake, H. (1990) Membrane-associated chromate reductase activity from *Enterobacter cloacae*. *J. Bacteriol.* **172**, 1670–1672
- Park, C. H., Keyhan, M., Wielinga, B., Fendorf, S., and Matin, A. (2000) Purification to homogeneity and characterization of a novel *Pseudomonas putida* chromate reductase. *Appl. Environ. Microbiol.* **66**, 1788–1795
- Ishibashi, Y., Cervantes, C., and Silver, S. (1990) Chromium reduction in *Pseudomonas putida*. *Appl. Environ. Microbiol.* **56**, 2268–2270
- Suzuki, T., Miyata, N., Horitsu, H., Kawai, K., Takamizawa, K., Tai, Y., and Okazaki, M. (1992) NAD(P)H-dependent chromium (VI) reductase of *Pseudomonas ambigua* G-1: a Cr(V) intermediate is formed during the reduction of Cr(VI) to Cr(III). *J. Bacteriol.* **174**, 5340–5345
- Kwak, Y. H., Lee, D. S., and Kim, H. B. (2003) *Vibrio harveyi* nitroreductase is also a chromate reductase. *Appl. Environ. Microbiol.* **69**, 4390–4395
- Aiyar, J., Berkovits, H. J., Floyd, R. A., and Wetterhahn, K. E. (1991) Reaction of chromium(VI) with glutathione or with hydrogen peroxide: Identification of reactive intermediates and their role in chromium(VI)-induced DNA damage. *Environ. Health Perspect.* **92**, 53–62
- Itoh, M., Nakamura, M., Suzuki, T., Kawai, K., Horitsu, H., and Takamizawa, K. (1995) Mechanism of chromium(VI) toxicity in *Escherichia coli*: is hydrogen peroxide essential in Cr(VI) toxicity? *J. Biochem.* **117**, 780–786
- Luo, H., Lu, Y., Shi, X., Mao, Y., and Delal, N. S. (1996) Chromium(VI)-mediated Fenton-like reaction causes DNA damage: implication to genotoxicity of chromate. *Ann. Clin. Lab. Sci.* **26**, 185–191
- Nies, A., Nies, D. H., and Silver, S. (1989) Cloning and expression of plasmid genes encoding resistance to chromate and cobalt in *Alcaligenes eutrophus*. *J. Bacteriol.* **171**, 5065–5070
- Ohtake, H., Cervantes, C., and Silver, S. (1987) Decreased chromate uptake in *Pseudomonas fluorescens* carrying a chromate resistance plasmid. *J. Bacteriol.* **169**, 3853–3856
- Bopp, L. H., Chakrabarty, A. M., and Ehrlich, H. L. (1983) Chromate resistance plasmid in *Pseudomonas fluorescens*. *J. Bacteriol.* **155**, 1105–1109
- Cervantes, C., and Ohtake, H. (1988) Plasmid-determined resistance to chromate in *Pseudomonas aeruginosa*. *FEMS Microbiol. Lett.* **56**, 173–176
- Summers, A. O., and Jacoby, G. A. (1978) Plasmid-determined resistance to boron and chromium compounds in *Pseudomonas aeruginosa*. *Antimicrob. Agents Chemother.* **13**, 637–640
- Cervantes, C., Ohtake, H., Chu, L., Misra, T. K., and Silver, S. (1990) Cloning, nucleotide sequence, and expression of the chromate resistance determinant of *Pseudomonas aeruginosa* plasmid pUM505. *J. Bacteriol.* **172**, 287–291
- Nies, A., Nies, D. H., and Silver, S. (1990) Nucleotide sequence and expression of a plasmid-encoded chromate resistance determinant from *Alcaligenes eutrophus*. *J. Biol. Chem.* **265**, 5648–5653
- Alvarez, A. H., Moreno-Sanchez, R., and Cervantes, C. (1999) Chromate efflux by means of the ChrA chromate resistance protein from *Pseudomonas aeruginosa*. *J. Bacteriol.* **181**, 7398–7400
- Bopp, L. H., and Erlich, H. L. (1988) Chromate resistance and reduction in *Pseudomonas fluorescens* strain LB300. *Arch. Microbiol.* **150**, 426–431
- Viamajala, S., Peyton, B. M., Sani, R. K., Apel, W. A., and Petersen, J. N. (2004) Toxic effects of chromium(VI) on anaerobic and aerobic growth of *Shewanella oneidensis* MR-1. *Biotechnol. Prog.* **20**, 87–95
- Qiu, X., Sundin, G. W., Wu, L., Zhou, J., and Tiedje, J. M. (2005) Comparative analysis of differentially expressed genes in *Shewanella oneidensis* MR-1 following exposure to UVC, UVB, and UVA radiation. *J. Bacteriol.* **187**, 3556–3564
- Myers, C. R., and Nealson, K. H. (1988) Bacterial manganese reduction and growth with manganese oxide as the sole electron acceptor. *Science* **240**, 1319–1321
- Brown, S. D., Martin, M., Deshpande, S., Seal, S., Huang, K., Alm, E., Yang, Y., Wu, L., Yan, T., Arkin, A., Chourey, K., Zhou, J., and Thompson, D. K. (2006) Cellular response of *Shewanella oneidensis* to strontium stress. *Appl. Environ. Microbiol.* **72**, 890–900
- Gao, H., Wang, Y., Liu, X., Yan, T., Wu, L., Alm, E., Arkin, A., Thompson, D. K., and Zhou, Z. (2004) Global transcriptome analysis of the heat shock response of *Shewanella oneidensis*. *J. Bacteriol.* **186**, 7796–7803
- Wan, X.-F., VerBerkmoes, N. C., McCue, L. A., Stanek, D., Connelly, H., Hauser, L. J., Wu, L., Liu, X., Yan, T., Leapart, A., Hettich, R. L., Zhou, J., and Thompson, D. K. (2004) Transcriptomic and proteomic characterization of the Fur regulon in the metal-reducing bacterium *Shewanella oneidensis*. *J. Bacteriol.* **186**, 8385–8400
- Schena, M., Shalon, D., Heller, R., Chai, A., Brown, P. O., and Davis, R. W. (1996) Parallel human genome analysis: microarray-based expression monitoring of 1000 genes. *Proc. Natl. Acad. Sci. U. S. A.* **93**, 10614–10619
- Eng, J. K., McCormack, A. L., and Yates, J. R., III (1994) An approach to correlate tandem mass spectral data of peptides with amino acid sequences in a protein database. *J. Am. Mass Spectrom.* **5**, 976–989
- Tabb, D. L., Hayes-McDonald, W., and Yates, J. R., III (2002) DTASelect and contrast: tools for assembling and comparing protein identifications from shotgun proteomics. *J. Proteome Res.* **1**, 21–26
- VerBerkmoes, N. C., Shah, M. B., Lankford, P. K., Pelletier, D. A., Strader, M. B., Tabb, D. L., McDonald, W. H., Barton, J. W., Hurst, G. B., Hauser, L., Davison, B. H., Beatty, J. T., Harwood, C. S., Tabita, F. R., Hettich, R. L., and Larimer, F. W. (2005) Determination and comparison of the baseline proteomes of the versatile microbe *Rhodospseudomonas palus-*

- tris under its major metabolic states. *J. Proteome Res.* **5**, 287–298
44. Heidelberg, J. F., Paulsen, I. T., Nelson, K. E., Gaidos, E. J., Nelson, W. C., Read, T. D., Eisen, J. A., Seshadri, R., Ward, N., Methe, B., Clayton, R. A., Meyer, T., Tsapin, A., Scott, J., Beanan, M., Brinkac, L., Daugherty, S., DeBoy, R. T., Dodson, R. J., Durkin, A. S., Haft, D. H., Kolonay, J. F., Madupu, R., Peterson, J. D., Umayam, L. A., White, O., Wolf, A. M., Vamathevan, J., Weidman, J., Impraim, M., Lee, K., Berry, K., Lee, C., Mueller, J., Khouri, H., Gill, J., Utterback, T. R., McDonald, L. A., Feldblyum, T. V., Smith, H. O., Venter, J. C., Nealson, K. H., and Fraser, C. M. (2002) Genome sequence of the dissimilatory metal ion-reducing bacterium *Shewanella oneidensis*. *Nat. Biotechnol.* **20**, 1118–1123
 45. Kolker, E., Picone, A. F., Galperin, M. Y., Romine, M. F., Higdon, R., Makarova, K. S., Kolker, N., Anderson, G. A., Qiu, X., Auberry, K. J., Babnigg, G., Beliaev, A. S., Edlefsen, P., Elias, D. A., Gorby, Y. A., Holzman, T., Klappenbach, J. A., Konstantinidis, K. T., Land, M. L., Lipton, M. S., McCue, L.-A., Monroe, M., Pasa-Tolic, L., Pinchuk, G., Purvine, S., Serres, M. H., Tsapin, S., Zakrajsek, B. A., Zhu, W., Zhou, J., Larimer, F. W., Lawrence, C. E., Riley, M., Collart, F. R., Yates, J. R., III, Smith, R. D., Giometti, C. S., Nealson, K. H., Fredrickson, J. K., and Tiedje, J. M. (2005) Global profiling of *Shewanella oneidensis* MR-1: expression of hypothetical genes and improved functional annotations. *Proc. Natl. Acad. Sci. U. S. A.* **102**, 2099–2104
 46. Ackerley, D. F., Gonzalez, C. F., Park, C. H., Blake, R., II, Keyhan, M., and Matin, A. (2004) Chromate-reducing properties of soluble flavoproteins from *Pseudomonas putida* and *Escherichia coli*. *Appl. Environ. Microbiol.* **70**, 873–882
 47. Shi, X. L., and Dalal, N. S. (1990) NADPH-dependent flavoenzymes catalyze one electron reduction of metal ions and molecular oxygen and generate hydroxyl radicals. *FEBS Lett.* **276**, 189–191
 48. Sumner, E. R., Shanmuganathan, A., Sideri, T. C., Willetts, S. A., Houghton, J. E., and Avery, S. V. (2005) Oxidative protein damage causes chromium toxicity in yeast. *Microbiology* **151**, 1939–1948
 49. Little, J. W. (1996) *Regulation of Gene Expression in Escherichia coli*, pp. 453–479. R. G. Landes Co., Georgetown, TX
 50. Kredich, N. M. (1996) *Escherichia coli* and *Salmonella typhimurium: Cellular and Molecular Biology*, 2nd Ed., pp. 514–527, American Society for Microbiology, Washington, D. C.
 51. Mihara, H., and Esaki, N. (2002) Bacterial cysteine desulfurases: their function and mechanisms. *Appl. Microbiol. Biotechnol.* **60**, 12–23
 52. Ram, R. J., VerBerkmoes, N. C., Thelen, M. P., Tyson, G. W., Baker, B. J., Blake, R. C., II, Shah, M., Hettich, R. L., and Banfield, J. F. (2005) Community proteomics of a natural microbial biofilm. *Science* **308**, 1915–1920
 53. Giometti, C. S., Khare, T., Tollaksen, S. L., Tsapin, A., Zhu, W., Yates, J. R., III, and Nealson, K. H. (2003) Analysis of the *Shewanella oneidensis* proteome by two-dimensional gel electrophoresis under nondenaturing conditions. *Proteomics* **3**, 777–785
 54. VerBerkmoes, N. C., Bundy, J. L., Hauser, L., Asano, K. G., Razumovskaya, J., Larimer, F., Hettich, R. L., and Stephenson, J. L., Jr. (2002) Integrating “top-down” and “bottom-up” mass spectrometric approaches for proteomic analysis of *Shewanella oneidensis*. *J. Proteome Res.* **1**, 239–252
 55. Liu, H., Sadygov, R. G., and Yates, J. R., III (2004) A model for random sampling and estimation of relative protein abundance in shotgun proteomics. *Anal. Chem.* **76**, 4193–4201
 56. Wang, C. C., and Newton, A. (1969) Iron transport in *Escherichia coli*: relationship between chromium sensitivity and high iron requirement in mutants of *Escherichia coli*. *J. Bacteriol.* **98**, 1135–1141
 57. Andrews, S. C., Robinson, A. K., and Rodríguez-Quiriones, F. (2003) Bacterial iron homeostasis. *FEMS Microbiol. Rev.* **27**, 215–237
 58. de Lorenzo, V., Perez-Martin, J., Escolar, L., Pesole, G., and Bertoni, G. (2004) *Iron Transport in Bacteria*, pp. 185–196, American Society for Microbiology, Washington, D. C.
 59. Andrews, S. C., Smith, J. M. A., Hawkins, C., Williams, J. M., Harrison, P. M., and Guest, J. R. (1993) Overproduction, purification and characterization of the bacterioferritin of *Escherichia coli* and a C-terminally extended variant. *Eur. J. Biochem.* **213**, 329–338
 60. Palma, M., DeLuca, D., Worgall, S., and Quadri, L. E. N. (2004) Transcriptome analysis of the response of *Pseudomonas aeruginosa* to hydrogen peroxide. *J. Bacteriol.* **186**, 248–252
 61. Salunkhe, P., Topfer, T., Buer, J., and Tummeler, B. (2005) Genome-wide transcriptional profiling of the steady-state response of *Pseudomonas aeruginosa* to hydrogen peroxide. *J. Bacteriol.* **187**, 2565–2572
 62. Zheng, M., Doan, B., Schneider, T. D., and Storz, G. (1999) OxyR and SoxRS regulation of *fur*. *J. Bacteriol.* **181**, 4639–4643
 63. Benov, L., Kredich, N. M., and Fridovich, I. (1996) The mechanism of the autotrophy for sulfur-containing amino acids imposed upon *Escherichia coli* by superoxide. *J. Biol. Chem.* **271**, 21037–21040
 64. Newton, G. L., Arnold, K., Price, M. S., Sherrill, C., Delcardayre, S. B., Aharonowitz, Y., Cohen, G., Davies, J., Fahey, R. C., and Davis, C. (1996) Distribution of thiols in microorganisms: mycothiol is a major thiol in most actinomycetes. *J. Bacteriol.* **178**, 1990–1995
 65. Mitaku, S., Hirokawa, T., and Tsuji, T. (2002) Amphiphilicity index of polar amino acids as an aid in the characterization of amino acid preference at membrane-water interfaces. *Bioinformatics* **18**, 608–616
 66. Ferguson, G. P., Töttemeyer, S., MacLean, M. J., and Booth, I. R. (1998) Methylglyoxal production in bacteria: suicide or survival? *Arch. Microbiol.* **170**, 209–219
 67. McGinnis, S., and Madden, T. L. (2004) BLAST: at the core of a powerful and diverse set of sequence analysis tools. *Nucleic Acids Res.* **32**, W20–W25
 68. Park, C. H., Gonzalez, C. F., Ackerley, D. F., Keyhan, M., and Matin, A. (2002) *Remediation and Beneficial Reuse of Contaminated Sediments*, pp. 103–111, Batelle Press, Columbus, OH
 69. Gonzalez, C. F., Ackerley, D. F., Lynch, S. V., and Matin, A. (2005) ChrR, a soluble quinone reductase of *Pseudomonas putida* that defends against H₂O₂. *J. Biol. Chem.* **280**, 22590–22595
 70. Dean, F., Krasnow, M. A., Otter, R., Matzuk, M. M., Spengler, S. J., and Cozzarelli, N. R. (1983) *Escherichia coli* type-1 topoisomerases: identification, mechanism, and role in recombination. *Cold Spring Harb. Symp. Quant. Biol.* **2**, 769–777
 71. Nurse, P., Levine, C., Hassing, H., and Mariani, K. J. (2003) Topoisomerase III can serve as the cellular decatenase in *Escherichia coli*. *J. Biol. Chem.* **278**, 8653–8660
 72. Plaper, A., Jenko-Brinovec, S., Premzl, A., Kos, J., and Raspor, P. (2002) Genotoxicity of trivalent chromium in bacterial cells. Possible effects on DNA topology. *Chem. Res. Toxicol.* **15**, 943–949
 73. Bencheikh-Latmani, R., Middleton Williams, S., Haucke, L., Criddle, C. S., Wu, L., Zhou, J., and Tebo, B. M. (2005) Global transcriptional profiling of *Shewanella oneidensis* MR-1 during Cr(VI) and U(VI) reduction. *Appl. Environ. Microbiol.* **71**, 7453–7460